EBioMedicine 74 (2021) 103734

Contents lists available at ScienceDirect

EBioMedicine

journal homepage: www.elsevier.com/locate/ebiom

Kynurenine induces T cell fat catabolism and has limited suppressive effects in vivo

Peter J. Siska[a], Jing Jiao[b], Carina Matos[a], Katrin Singer[c], Raffaela S. Berger[d], Katja Dettmer[d], Peter J. Oefner[d], Michelle D. Cully[b], Zhonglin Wang[e], William J. Quinn III[f], Kristen N. Oliff[g], Benjamin J. Wilkins[h], Lanette M. Christensen[i], Liqing Wang[i], Wayne W. Hancock[i], Joseph A. Baur[f], Matthew H. Levine[e], Ines Ugele[c], Roman Mayr[j], Kathrin Renner[a,k], Liang Zhou[g], Marina Kreutz[a,k], Ulf H. Beier[b,l,*]

[a] Department of Internal Medicine III, University Hospital Regensburg, 93053 Regensburg, Germany
[b] Division of Nephrology, Department of Pediatrics, Children's Hospital of Philadelphia, and University of Pennsylvania, Philadelphia, PA 19104, USA
[c] Department of Otorhinolaryngology, University Hospital Regensburg, 93053 Regensburg, Germany
[d] Institute of Functional Genomics, University of Regensburg, 93053 Regensburg, Germany
[e] Department of Surgery, Penn Transplant Institute, Perelman School of Medicine, Children's Hospital of Philadelphia and University of Pennsylvania, Philadelphia, PA 19104, USA
[f] Department of Physiology and Institute of Diabetes, Obesity, and Metabolism, University of Pennsylvania, Philadelphia, PA 19104, USA
[g] Department of Infectious Diseases and Immunology, College of Veterinary Medicine, University of Florida, Gainesville, FL 32608, USA
[h] Division of Anatomic Pathology, Department of Pathology and Laboratory Medicine, Children's Hospital of Philadelphia, Philadelphia, PA 19104 USA
[i] Division of Transplant Immunology, Department of Pathology and Laboratory Medicine, and Biesecker Center for Pediatric Liver Disease, Children's Hospital of Philadelphia and University of Pennsylvania, Philadelphia, PA 19104, USA
[j] Department of Urology, Caritas St. Josef Medical Centre, University of Regensburg, Regensburg, Germany
[k] Regensburg Center for Interventional Immunology, University of Regensburg, 93053 Regensburg, Germany
[l] Current affiliation: Janssen Research and Development, Spring House, 19477 PA, USA

ARTICLE INFO

Article History:
Received 13 August 2021
Revised 18 November 2021
Accepted 21 November 2021
Available online 4 December 2021

Keywords:
T cell metabolism
immunosuppression
tumour microenvironment
indoleamine-2,3-dioxygenase
cancer metabolism
aryl hydrocarbon receptor

ABSTRACT

Background: L-kynurenine is a tryptophan-derived immunosuppressive metabolite and precursor to neurotoxic anthranilate and quinolinate. We evaluated the stereoisomer D-kynurenine as an immunosuppressive therapeutic which is hypothesized to produce less neurotoxic metabolites than L-kynurenine.
Methods: L-/D-kynurenine effects on human and murine T cell function were examined in vitro and in vivo (homeostatic proliferation, colitis, cardiac transplant). Kynurenine effects on T cell metabolism were interrogated using [^{13}C] glucose, glutamine and palmitate tracing. Kynurenine was measured in tissues from human and murine tumours and kynurenine-fed mice.
Findings: We observed that 1 mM D-kynurenine inhibits T cell proliferation through apoptosis similar to L-kynurenine. Mechanistically, [^{13}C]-tracing revealed that co-stimulated CD4^{+} T cells exposed to L-/D-kynurenine undergo increased β-oxidation depleting fatty acids. Replenishing oleate/palmitate restored effector T cell viability. We administered dietary D-kynurenine reaching tissue kynurenine concentrations of 19 μM, which is close to human kidney (6 μM) and head and neck cancer (14 μM) but well below the 1 mM required for apoptosis. D-kynurenine protected Rag1$^{-/-}$ mice from autoimmune colitis in an aryl-hydrocarbon receptor dependent manner but did not attenuate more stringent immunological challenges such as antigen mismatched cardiac allograft rejection.
Interpretation: Our dietary kynurenine model achieved tissue concentrations at or above human cancer kynurenine and exhibited only limited immunosuppression. Sub-suppressive kynurenine concentrations in human cancers may limit the responsiveness to indoleamine 2,3-dioxygenase inhibition evaluated in clinical trials.

Abbreviations: IDO, indoleamine 2,3-dioxygenase; TDO, tryptophan 2,3-dioxygenase; HNSCC, head and neck squamous cell carcinoma; RCC, renal clear cell carcinoma; AhR, aryl hydrocarbon receptor; DSS, dextran sodium sulphate; LC-MS, liquid chromatography- mass spectrometry; TiPARP, Tetrachlorodibenzo-p-dioxin (TCDD)-inducible poly(ADP-ribose) polymerase

* Correspondence: Dr. Ulf H. Beier
E-mail address: ubeier@its.jnj.com (U.H. Beier).

https://doi.org/10.1016/j.ebiom.2021.103734

Funding: The study was supported by the NIH, the Else Kröner-Fresenius-Foundation, Laffey McHugh foundation, and American Society of Nephrology.

Research in context

Evidence before this study

L-kynurenine is a breakdown product of the amino acid L-tryptophan generated through the enzymes tryptophan- and indoleamine 2,3-dioxygenase (IDO). L-kynurenine has been associated with neurotoxicity and suppression of immune responses against cancers. IDO has been found expressed in some human cancers which have also tryptophan depletion and kynurenine enrichment. Mechanistically, expressing IDO in tumours implanted into mice made those tumours resistant to T cell-mediated anti-cancer immune responses. Kynurenine and derivative metabolites have been shown to cause cell death in T cells and can impair T cells through the aryl hydrocarbon receptor. This has led to IDO inhibitor development to treat cancer. Unfortunately, IDO inhibitors have failed to show therapeutic benefits against cancer in clinical trials so far.

Added value of this study

Human head and neck as well as renal carcinoma tissue specimens exhibited low micromolar kynurenine concentrations which were at or even below tissue levels of kynurenine achieved by feeding mice 300 mg/kg/d kynurenine in their diet. At these concentrations, only weak aryl hydrocarbon receptor signalling dependent immunosuppressive effects were observed. T cells exposed to kynurenine activate fatty acid β-oxidation, leading to fatty acid depletion. This could explain the apoptosis phenotype seen with T cells exposed to kynurenine in cell culture. Standard cell culture media contain only a limited amount of lipids which is different from most in vivo conditions. Adding fatty acids to the cell culture media prevents kynurenine-induced T cell apoptosis. Together, these new data raised a suspicion that the importance of kynurenine as an immunosuppressive metabolite may have been overrated in the cancer literature.

Implications of all the available evidence

IDO targeting remains a hot topic in cancer immunotherapy and tumour metabolism. There are ongoing clinical trials with patients who may not benefit from IDO inhibition. Stratification of patients based on tumour tissue kynurenine concentration measurements might improve risk-benefit assessment of IDO inhibition in clinical trials.

1. Introduction

L-kynurenine is derived from L-tryptophan through indoleamine and tryptophan 2,3-dioxygenases (IDO, TDO). L-kynurenine is perhaps best known as a precursor for NAD^+ de novo biosynthesis [1]. It also plays an important role in neurologic disorders, cancer and inflammation. L-kynurenine has reported immunosuppressive properties, which are mediated through T cell apoptosis and regulatory T cell (Treg) induction. Kynurenines also function as agonists via the immunosuppressive aryl hydrocarbon receptor (AhR) [2-6]. Several tumours, such as glioblastoma, head and neck squamous cell carcinoma (HNSCC), and renal clear cell carcinoma (RCC), among many others, express IDO/TDO that is thought to suppress anti-tumour immunity through L-kynurenine production acting as a metabolic barrier to successful anti-neoplastic therapy [7-9]. This has led to a great interest in developing IDO-inhibitors for cancer treatment, but respective clinical trials have performed poorly [10].

The reported immunosuppressive effects of L-kynurenine have led us to question if this metabolite could be exploited for therapeutic immunosuppression. This has been done successfully with L-lactic acid, be it through the adoptive transfer of lactic acid producing dendritic cells [11] or bacteria [12], or direct injection with pH neutral sodium L-lactate [13-14]. Lactate is generally well tolerated at high doses and is commonly used in intravenous fluids, such as Ringer's lactate solution (28 mmol/L) or peritoneal dialysis fluid (40 mmol/L). However, for L-kynurenine this is not an option. L-kynurenine derived anthranilic acid, 3-hydroxykynurenine, 3-hydroxyanthranilic acid and quinolinic acid act as N-methyl-d-aspartate (NMDA) receptor agonists, induce free radical production, and are associated with epilepsy, amyotrophic lateral sclerosis, Huntington's disease, Parkinson's disease, Alzheimer's disease, and multiple sclerosis [15]. Therefore, in contrast to lactate, administering large quantities of L-kynurenine does not seem suitable as an immunosuppressive strategy.

In contrast to L-kynurenine, its enantiomer D-kynurenine has been suggested to being resistant to kynureninase, thus bypassing most of the aforementioned neurotoxic metabolites (**Figure 1a**) [16,17]. D-kynurenine contributes to kynurenine derivatives independent of kynureninase such as kynurenic acid, but these are not associated with toxicity. In fact, kynurenic acid even has neuroprotective properties [15,18], and kynureninase inhibition is a neuroprotective treatment strategy to shunt kynurenine metabolites away from quinolinic acid to kynurenic acid [19,20]. Under these assumptions, D-kynurenine could potentially be a therapeutically interesting immunosuppressive metabolite. We have evaluated D-kynurenine's immunosuppressive effects and examined its mechanism compared to L-kynurenine. Our findings may improve the understanding of kynurenine's immunosuppressive effects, and may also shed some light on why pharmacologic IDO inhibition has been unsuccessful in cancer treatment [10].

2. Methods

2.1. Ethics statement

All healthy blood donors and tumour patients gave written informed consent as approved by the Institutional Review Board at the University of Pennsylvania (healthy donors: IRB 70906) and ethical committee of the University Hospital Regensburg (healthy donors: 13-101-0240; RCC: 08/108; and HNSCC: 12-101-0070) in accordance with the Declaration of Helsinki. Mice were studied using protocols approved by the Institutional Animal Care and Use Committees of the Children's Hospital of Philadelphia and University of Pennsylvania (19-000561 and 20-000746) and equivalent committees at the University of Regensburg and the University of Florida, Gainesville (201808674 and 202108674).

2.2. Human T cell donors and tumour patients

Human T cells were obtained from de-identified adult male and female healthy donors at both the University of Pennsylvania and the University Hospital of Regensburg. Serum and tissues

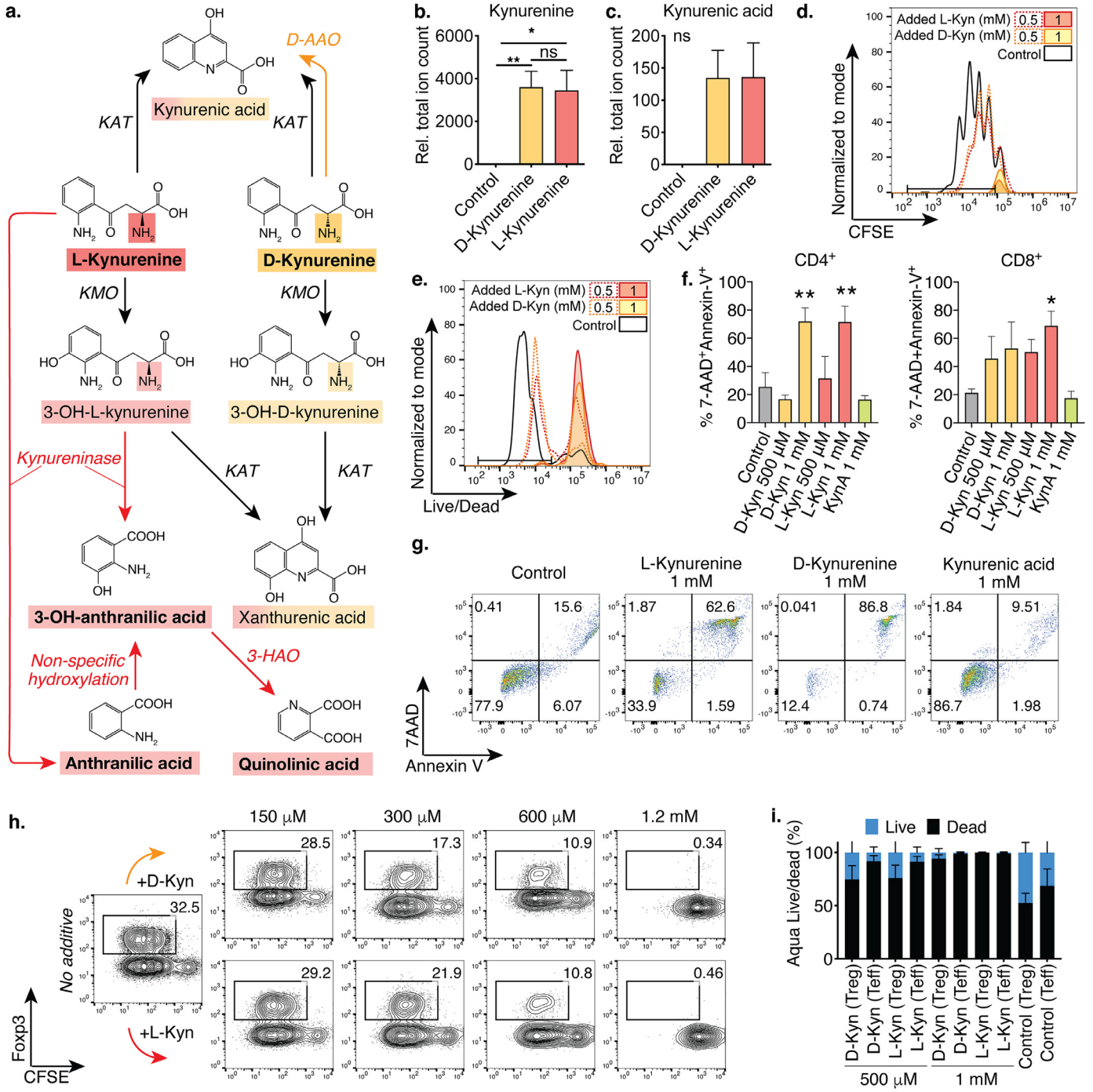

Figure 1. L- and D-kynurenine cause comparable apoptosis in human and murine T cells. (**a**) Schematic comparing L- and D-kynurenine metabolism. (**b, c**): Murine CD4$^+$CD25$^-$ Tconv were co-stimulated overnight with CD3ε/CD28 mAb coated beads overnight, and then exposed to 1 mM D- or L-kynurenine or H_2O control. Metabolites were extracted and analysed by LC-MS and displayed as total ion count relative to the H_2O control. (**b**) Both kynurenine (Kyn) enantiomers were imported into T cells, and (**c**) kynurenic acid (KynA) was produced. Data pooled from 11 and 6 independent experiments, respectively (one-way ANOVA with Tukey's multiple comparison test). (**d, e**) Murine Tconv were CFSE-labelled and stimulated with anti-CD3ε and irradiated antigen presenting cells. After three days, proliferation was assessed by flow cytometry. Experiment representative of six independent replicates. (**f, g**) Human T cells were co-stimulated using CD3ε/CD28 mAb coated beads for three days, with added kynurenine or KynA. After two days, apoptosis was assessed by flow cytometry. (**f**) Quantitative data pooled from three independent experiments (one-way ANOVA with Fisher's LSD) and (**g**) representative CD4$^+$ T cell apoptosis data. (**h**) Murine Tconv cells were CFSE-labelled and co-stimulated and polarized to induce Foxp3 by adding IL-2 and TGF-β. After four days, Foxp3 expression in CD4$^+$ T cells was assessed. D-/L-kynurenine did not increase Foxp3 expression. Data representative of three independent experiments. (**i**) Tconv were co-stimulated with anti-CD3ε and irradiated antigen presenting cells and co-cultured with Treg at a 2:1 ratio. After three days, Treg and Tconv cell viability was assessed using Aqua Live/Dead. Data pooled from three independent experiments. Abbreviations: D-AAO, D-amino acid oxidase; KAT, Kynurenine aminotransferase; KMO, Kynurenine 3-monooxygenase; 3-HAO; 3-Hydroxyanthranilate oxidase; Kyn, Kynurenine; KynA, Kynurenic acid. * and ** indicate $p<0.05$ and $p<0.01$, respectively. Data shown as mean with SEM (**b, c, f, i**).

from 6 renal cell carcinoma (RCC) patients and 27 head and neck squamous cell carcinoma (HNSCC) patients treated at the University Hospital Regensburg were included. For analyses of the tumour metabolome, tumour and healthy tissues were surgically removed and immediately placed in liquid nitrogen and then cryopreserved until analysis.

2.3. Mice

We purchased B6/Rag1$^{-/-}$, C57BL/6J, and BALB/c from The Jackson Laboratory (Bar Harbor, ME) or Charles River (Germany). AhR$^{-/-}$ [21], as well as AhR$^{+/-}$, and AhR$^{+/+}$ littermate control mice on a C57BL/6J background were bred at the University of Florida, Gainesville. All mice were housed under pathogen-free conditions.

2.4. Reagents and resources

Reagents and resources are summarized in **supplemental table S1**.

2.5. Cell culture media and conditions

For standard cell culture medium for murine and U.S. human T cell experiments, we used RPMI 1640 medium supplemented with 10% foetal bovine serum (FBS), penicillin (100 U $\times$ mL^{-1}), streptomycin (100 μg $\times$ mL^{-1}), and 55 nM β_2-mercaptoethanol. For German human T cell experiments we used RPMI 1640 with 5% human AB serum (2-10% in some experiments as indicated), 2 mM L-glutamine, 50 U $\times$ mL^{-1} penicillin, and 50 μg $\times$ mL^{-1} streptomycin. For [^{13}C] tracing experiments, we used Agilent Seahorse XF base medium (cat. #102353-100) from Agilent Technologies (Santa Clara, CA) and added 10% dialyzed foetal bovine serum (cat. #26400036) from Thermo Fisher Scientific (Waltham, MA) and 10 mM $NaHCO_3$ for buffering, to which glucose/glutamine and palmitate were added as indicated. For bioenergetic measurements, we used Seahorse XF base medium (cat. #102353-100) from Agilent Technologies plus 10 mM D-glucose, 1 mM sodium pyruvate, and 2 mM L-glutamine (without pyruvate/glucose for glycolytic stress test). Cells were cultured at 37°C with 5% CO_2, except for cells plated prior to Seahorse assays, which required incubation without CO_2.

2.6. Special mouse diet

In order to provide constant D-kynurenine intake, we had a D-kynurenine diet made by Research Diets, Inc. (New Brunswick, NJ). We determined the diet dose of kynurenine through the following formula:

$$DD = \left(SD \times \frac{BW}{FI}\right), with$$

DD, diet dose (calculated as 1,500 mg D-kynurenine/kg chow)
SD, desired single daily dose of D-kynurenine (300 mg/kg/d)
BW, body weight (20 grams, estimated starting weight)
FI, food intake, estimated ~4 grams/day C57BL/6 mice [22]

As a precaution to avoid unequal administration, we included only mice with less than 0.5 gram difference in starting body weight between experimental groups at the start of the experiment. Nutritional details of the D-kynurenine enriched diet (product #**D19101801**) and its control diet (product #**D11112201**) are shown in **Table 1**.

2.7. General experimental design and blinding

The surgeon performing the cardiac transplants and measuring allograft survival (Z.W.) was blinded to and unaware of the treatment conditions. The pathologist (B.J.W.) evaluating tissue samples was blinded to and unaware of the treatment conditions. Staff attending the mice on the kynurenine diet could identify the type of diet based upon food coloring which was necessary to ensure that the correct diet was administered. For weight-based outcomes, mice were assembled into groups to ensure equal starting weights (in addition to normalization to the starting weight). Details on age and gender of animals are discussed in each in vivo model below.

2.8. Bioenergetic measurements

We measured bioenergetic function as oxygen consumption rate (OCR) and extracellular acidification rate (ECAR) using a XF96 analyser (Seahorse Biosciences, North Billerica, MA). For our T cells studies, XF96 plates were coated using Cell-Tak (BD Biosciences, Franklin Lakes, NJ) as previously reported [23]. Isolated T cells were plated in unbuffered XF assay media, and then incubated for 30-60 min at 37°C without CO_2. For our T cell studies, we used 2 $\times$ 10^5 cells per well for XF96 assays. To enhance cell adherence, plates were spun at room temperature for 5 min at 400 g. Three baseline measurements of OCR and ECAR were taken and then the cells were exposed to oligomycin A, cyanide-4-[trifluoromethoxy]phenylhydrazone (FCCP) and rotenone and/or antimycin A. We used 1.25 μM oligomycin, 0.5 μM FCCP, and 1 μM rotenone & antimycin A, or ECAR (with final concentrations of 10 mM glucose, 2 μM oligomycin, and 50 mM 2-deoxy-D-glucose). Three readings were taken after each sequential injection. Instrumental background was measured in separate control wells using the same conditions without biological material. Data were analysed using Wave (Agilent), Excel and Prism. Cell culture oxygen consumption experiments were performed using the SDR SensorDish® Reader (PreSens Precision Sensing GmbH, Regensburg, Germany) equipped with optical oxygen (OxoDish®) or hydrogen (HydroDish) sensors. CD4$^+$CD25$^-$ human T cells were cultured for 4 days and oxygen consumption was recorded in real time at 5 min intervals. Data were analysed using Excel and Prism.

2.9. Cardiac Allografting

For cardiac allografting, we transplanted BALB/c hearts (H-2^d) into the abdomen of C57BL/6J recipients (H-2^b). We used female recipients and donors between 8-12 weeks of age, randomly assigned to treatment groups. We chose female mice to minimize fight injuries and age 8-12 weeks to ensure sufficiently large blood vessels for microsurgery. Recipients received low-dose rapamycin (0.5 mg $\times$ kg^{-1} $\times$ day^{-1}) via ALZET® pumps, and either D-kynurenine diet or control chow. Sample sizes were determined based upon effect size of the primary outcome mismatched cardiac allograft survival determined by palpation, and experience with the BALB/c to C57BL/6J cardiac transplant model [23,24]. Allograft survival was assessed by daily palpation. Mice were offered either D-kynurenine diet or control chow. A priori exclusion criteria included death during or up to 24 hours after cardiac transplant surgery which did not occur. No animals were excluded from the analysis.

2.10. Colitis

We utilized two colitis models, B6/Rag1$^{-/-}$ adoptive transfer colitis, as well as a dextran sodium sulfate (DSS-) induced colitis model. In the B6/Rag1$^{-/-}$ adoptive transfer colitis model, 9-10 weeks old B6/Rag1$^{-/-}$ mice were adoptively transferred i.v. with 10^6 CD4$^+$CD25$^-$ Tconv cells from C57BL/6J donors. Mice were observed for weight, gross blood in their stool, and other clinical parameters as previously reported [25]. Sample sizes were determined based upon effect size of the primary outcome weight loss and prior experience with the colitis models [25]. For the adoptive transfer colitis experiment with AhR knockout donors, spleens of AhR$^{-/-}$, AhR$^{+/-}$ and AhR$^{+/+}$ littermate controls were collected at the University of Florida and sent overnight in PBS on ice, and T cells were isolated the next morning. The genotype of the donor mice was separately confirmed (Figure S3a, b). To assess colitis induced by DSS, we used 5% DSS (wt/vol, with a molecular weight 36-50 kDa, Cat. #160110, MP Biomedicals, Solon, OH), using a previously published chronic colitis model involving multiple repetitive cycles of 5% DSS designed to assess Th1 based immunopathology [25,26]. Briefly, 12-week-old female C57BL/6J mice (5 per group, randomly selected, and confirmed to have near

Table 1
D-kynurenine diet composition

Research Diets, Inc. Product #	D11112201		D19101801	
	Control diet		1500 mg D-kynurenine per kg diet	
	gram%	kcal%	gram%	kcal%
Protein	19	20	19	20
Carbohydrate	63	65	63	65
Fat	7	15	7	15
Total		100		100
kcal/gm	3.81		3.81	
Ingredient	**gram**	**kcal**	**gram**	**kcal**
Casein	200	800	200	800
L-Cystine	3	12	3	12
Corn starch	381	1524	381	1524
Maltodextrin 10	110	440	110	440
Dextrose	150	600	150	600
Cellulose, BW200	75	0	75	0
Inulin	25	37.5	25	37.5
Soybean oil	70	630	70	630
Mineral mix S10026 (w/ o Ca, P, or K)	10	0	10	0
Dicalcium phosphate	13	0	13	0
Calcium carbonate, light, USP	5.5	0	5.5	0
Potassium citrate, 1 H_2O	16.5	0	16.5	0
Vitamin Mix V10001	10	40	10	40
Choline bitartrate	2	0	2	0
D-kynurenine	0	0	1.609	0
Yellow dye #5, FD&C	0.025	0	0	0
Red dye #40, FD&C	0	0	0.05	0
Blue dye #1, FD&C	0.025	0	0	0
Total	**1071.05**	**4084**	**1072.659**	**4084**
D-kynurenine (mg/kg diet)	0		1500.0	

equal starting weight with no significant difference between groups) received cycling doses of 5% DSS interchanged with normal drinking water every five to seven days (see Figure 2l), for a total observation period of 40 days. Female mice were chosen to eliminate fight wounds between animals potentially compromising inflammatory readouts, and a uniform age of 12 weeks was required to exclude somatic weight gain and standardize weight loss observations. Mice were offered either D-kynurenine diet or control chow after the initial DSS exposure. A priori exclusion criteria were not set. No animals were excluded from the analysis.

2.11. Cell isolation, T cell function and flow cytometry

Murine spleen and peripheral lymph nodes were harvested and processed to obtained single cell suspensions of lymphocytes. Red blood cells were removed by hypotonic lysis. We used magnetic beads (Miltenyi Biotec, San Diego, CA) for isolation of Tconv ($CD4^+CD25^-$), Treg ($CD4^+CD25^+$), cytotoxic T cells ($CD8^+$), and antigen presenting cells ($CD90.2^-$). Human $CD4^+$ and $CD8^+$ T cells were purified using magnetic beads. Purified T cells were stimulated and stained with 7AAD and Annexin-V to assess cell death. In some experiments, human PBMC were stimulated and stained with anti-CD4 and anti-CD8 antibodies. For mixed leukocyte reactions, we generated immature dendritic cells from human blood monocytes. Monocytes were cultured in culture flasks at a concentration of 1×10^6 cells per 1.5 mL in RPMI 1640 for five days with 10% foetal calf serum (FCS), 225 U/mL granulocyte macrophage colony stimulating factor (Peprotech, Hamburg, Germany), and 144 U $\times$ mL^{-1} recombinant IL-4 (Peprotech). Next, we co-cultured 10,000 induced dendritic cells with 100,000 allogeneic CFSE-labelled human $CD4^+$ T lymphocytes in RPMI containing 5% AB serum, L-glutamine (2 mM), penicillin (50 U $\times$ mL^{-1}), and streptomycin (50 μg $\times$ mL^{-1}). Cells were cultured in round bottom 96-well plates, in the presence of defined L- and D-kynurenine concentrations, in a final volume of 200 μL. Lipopolysaccharide was added to induce dendritic cell maturation. On day 6, cells were harvested, counted and analysed by flow cytometry. All flow cytometry data was captured using Cyan (Dako), Cytoflex (Beckman Coulter, Brea, CA) and LSR-Fortessa (BD) and analysed using the FlowJo 10.2 software.

2.12. Histology

Segments of bowel that included small intestine, terminal ileum, and colon were fixed in 10% neutral buffered formalin, paraffin-embedded, and haematoxylin and eosin-stained sections (4 μm) were reviewed by a pathologist (B.J.W.) blinded to treatment conditions. Histologic findings were characterized using a previously published scoring system [25] to include the following parameters: (1) degree of lamina propria inflammation graded 0-3; (2) degree of mucin depletion as evidenced by loss of goblet cells graded 0-2; (3) reactive epithelial changes (nuclear hyperchromatism, random nuclear atypia, increased mitotic activity) graded 0-3; (4) number of intraepithelial lymphocytes per high power field within crypts graded 0-3; (5) degree of crypt architectural distortion graded 0-3; (6) degree of inflammatory activity (infiltration of neutrophils within lamina propria and crypt epithelium, "cryptitis") graded 0-2; (7) degree of transmural inflammation graded 0-2; and (8) degree of mucosal surface erosion up to total surface ulceration graded 0-2. For display in heatmaps, the histological score was normalized to a scale of 0-100%.

2.13. Homeostatic proliferation

To assess the effect of L- and D-kynurenine on T cell function in vivo, we adoptively transferred 1×10^6 $CD90.1^+$ $CD4^+CD25^-$ conventional T cells into 8-week-old female B6/$RAG1^{-/-}$ mice through intraperitoneal injection. Mice were randomly assigned to the treatment groups, either 30 mg $\times$ kg^{-1} $\times$ d^{-1} L- or D-kynurenine or water control (Figure 2a). Female mice were chosen to prevent fight wounds in the B6/$RAG1^{-/-}$ mice potentially compromising inflammatory readouts. Sample sizes were determined based upon prior experience on effect size of the primary outcome T cell homeostatic proliferation in the Thy1.1 homeostatic proliferation model [25,27]. Splenocytes were obtained on day 25, quantified, and CD90.1, CD4 and Foxp3 were assessed by flow cytometry as previously reported [27]. A priori exclusion criteria were not set. No animals were excluded from the analysis.

2.14. Metabolite extraction and derivatization

Cells were harvested in 1 mL medium and washed with 10 mL ice cold Hanks' Balanced Salt Solution (Thermo Fisher) with 8 mM D-glucose. Cells were quickly spun down (1,600 rpm, equivalent to 558.1 g, for 1 min, Heraeus X3R Multifuge, Thermo Fisher), and then decanted and extracted with a −20°C pre-cooled mixture of methanol, acetonitrile, and water with 0.5% formic acid (all HPLC grade) at a ratio of 40:40:20, respectively. The extracted samples were then vortexed, and 1.2 mL transferred into an Eppendorf tube and then incubated on ice for 5 minutes. The samples were centrifuged (558.1 g, for 20 sec) at 4°C, the supernatant neutralized with NH_4HCO_3 to pH 7 and immediately frozen at −80°C until analysis. For the assessment of glycolytic intermediates in activated Teff in the [^{13}C] tracing experiments, rapid processing is essential. Here, we modified the extraction to process one sample at a time, which was rapidly spun in a 4°C pre-cooled centrifuge (Eppendorf 5415D at 13,200 rpm, equivalent to 14,227.2 g, for 20 seconds, including acceleration time). Subsequently, the sample was rapidly decanted and placed on dry ice. The cell pellet was then mixed and suspended in the above mentioned −20°C pre-cooled extraction buffer made of methanol, acetonitrile, and water with 0.5% formic acid (all HPLC grade) at a ratio of

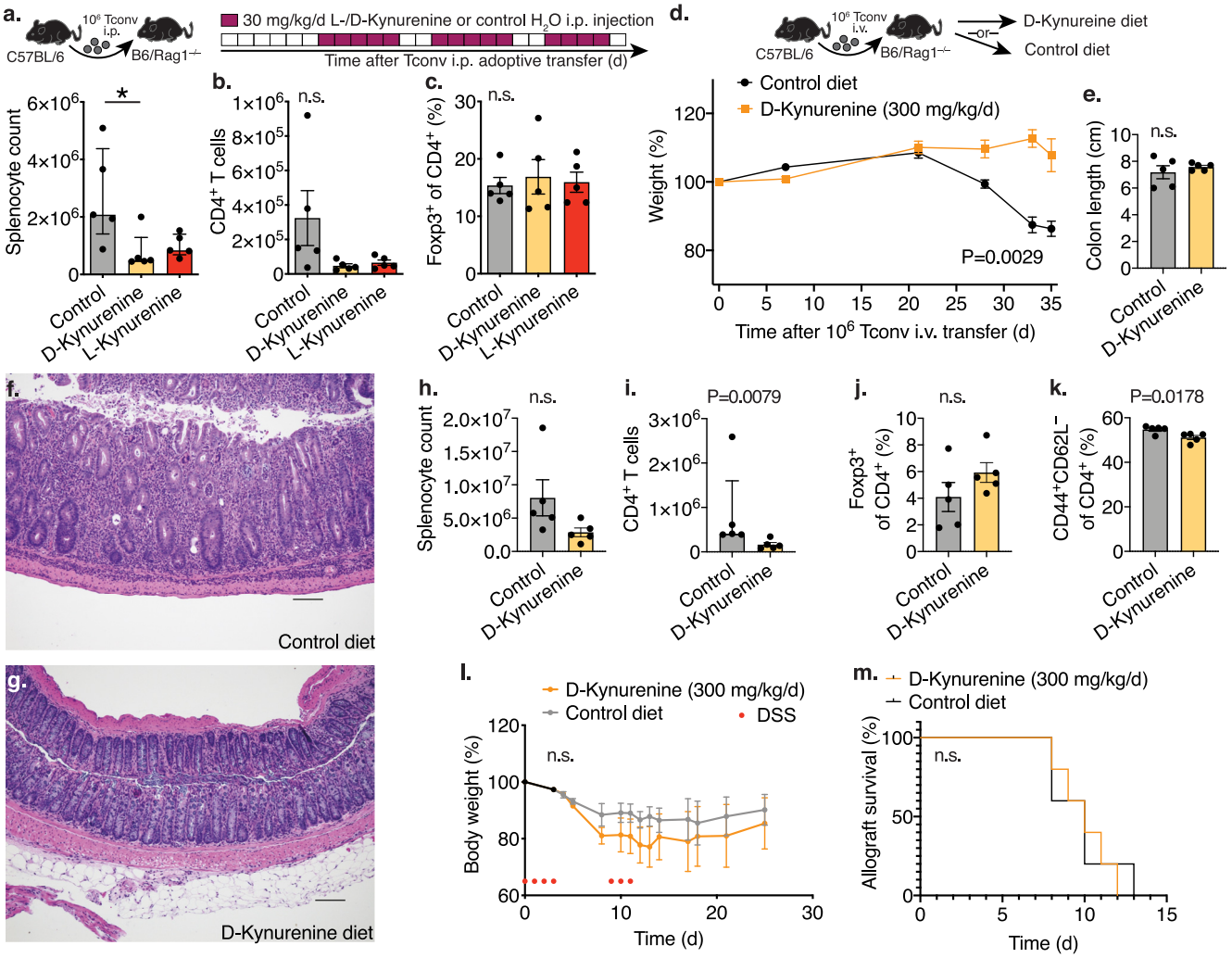

Figure 2. D-kynurenine alleviates adoptive transfer colitis but does not prevent MHC-mismatched allograft rejection or dextran sodium sulphate induced colitis. (**a-c**) Homeostatic proliferation: C57BL/6J 1 × 10^6 Tconv were injected intraperitoneally (i.p.) into B6/Rag1$^{-/-}$ mice. The recipient mice were treated with 30 mg/kg/d L-/D-kynurenine or water i.p. at the indicated timepoints (5/group). After 25 days, splenocytes were assessed by flow cytometry. (**a**) Kruskal Wallis test with Dunn's multiple comparison test, (**b, c**) one-way ANOVA with Tukey's multiple comparison test. (**d-k**) Adoptive transfer colitis. B6/Rag1$^{-/-}$ mice were adoptively transferred with C57BL/6J 1 × 10^6 Tconv intravenously (i.v.) and received either 300 mg/kg/d D-kynurenine enriched or control chow (5/group). (**d**) Weight curve normalized to starting weight (area under the curve, unpaired t-test). (**e**) Colon length at the end of the experiment (unpaired t-test). (**f, g**) Histology of colon specimens from B6/Rag1$^{-/-}$ mice after Tconv adoptive transfer. Haematoxylin and eosin staining; scale bar 100 μm. (**f**) B6/Rag1$^{-/-}$ mice fed on a control diet developed significant colitis with mucosal and focally transmural neutrophilic infiltration including crypt abscesses, and crypt architectural distortion. (**g**) In contrast, B6/Rag1$^{-/-}$ mice receiving D-kynurenine supplementation showed preserved colonic mucosal architecture with patchy mild inflammatory activity. (**h-k**) Flow cytometry of splenocytes. (**l**) C57BL/6J mice received 5% dextran sodium sulfate (DSS) in the drinking water at the indicated time points (red dots, 5/group) and either 300 mg/kg/d D-kynurenine enriched or control chow (5/group, two-way ANOVA with Bonferroni's multiple comparison test). (**m**) MHC-mismatched BALB/c hearts were transplanted into the abdomen of C57BL/6J recipients, which received 0.5 mg/kg/d rapamycin through osmotic ALZET® pumps, and either 300 mg/kg/d D-kynurenine enriched or control chow (5/group, Log-rank (Mantel-Cox) test. * indicates $p<0.05$. Data shown as median with IQR (**a, i**) or mean with SEM (**b, c, d, e, h, j, k, l**).

40:40:20, respectively. The samples were subsequently centrifuged (Eppendorf 5415D at 13,200 rpm, equivalent to 14,227.2 g, for 20 seconds, including acceleration time), neutralized with NH_4HCO_3 to pH 7, and immediately frozen at −80°C until analysis.

2.15. Liquid chromatography-mass spectrometry

Cell extracts were analysed by liquid chromatography-mass spectrometry mass spectrometry (LC-MS) using a Q Exactive PLUS hybrid quadrupole-orbitrap mass spectrometer (Thermo Scientific) coupled to hydrophilic interaction liquid chromatography (HILIC) via electrospray ionization. The LC separation was performed on a XBridge BEH Amide column (150 mm × 2.1 mm, 2.5 μm particle size, Waters, Milford, MA) using a gradient of solvent A (95%:5% H_2O:acetonitrile with 20 mM ammonium acetate, 20 mM ammonium hydroxide, pH 9.4), and solvent B (100% acetonitrile). The gradient was 0 min – 2 min, 85% B; 3 min, 80% B; 5 min, 80% B; 6 min, 75% B; 7 min, 75% B; 8 min, 70% B; 9 min, 70% B; 10 min, 50% B; 12 min, 50% B; 13 min, 25% B; 16 min, 25% B; 18 min, 0% B; 23 min, 0% B; 24 min, 85% B; 30 min, 85% B. The flow rate was 150 μL × min^{-1}. Injection volume was 10 μL and autosampler and column temperature were 4°C and 25°C, respectively. The MS scans were in negative ion mode with a resolution of 70,000 at m/z 200. The automatic gain control (AGC) target was 5 × 10^5 and the scan range was 75–1,000 at 1 Hz. Data were analysed using MAVEN software [28]. Isotope labelling was corrected for natural abundance of [^{13}C] using an in-house correction code in R [29].

Tissue samples for the analysis of tryptophan, kynurenine and kynurenic acid were immediately frozen in liquid nitrogen after resection. Samples were processed as described previously [30]. In

brief, tissues were weighted, and care was taken to keep the tissues frozen. Then, tissues were homogenized in 80% methanol using Precellys vials with 1.4 mm ceramic beads. During extraction an internal standard mix was added to the samples that contained stable isotope labelled analogues of the target analytes for quantification. Tissue extracts were evaporated and reconstituted in water with formic acid. Tryptophan metabolites were measured in the extracts by liquid chromatography-tandem mass spectrometry (HPLC-MS/MS) [31]. Quantification was achieved using a calibration curve for each analyte based on the peak area ratio of analyte to stable isotope labelled analogue. Analyte amounts in the extracted tissue were normalized to tissue weight.

2.16. RNA analysis

RNA was extracted using RNeasy kits (Qiagen, Hilden, Germany), and RNA integrity and quantity were analysed by photometry (Nanodrop 2000, Thermo Fischer). Revere transcription and qPCR were performed as reported [27]. Isolated RNA was reverse transcribed to cDNA with random hexamers and amplified (PTC-200; MJ Research). For the U87-MG glioblastoma samples, 4×10^5 cells per well were seeded in 6-well plates and incubated for 24 h prior to treatment with kynurenine or DMSO as carrier control. After 24 h, cells were harvested, and total RNA was isolated using the RNeasy Mini Kit (Qiagen) followed by cDNA synthesis using the High Capacity cDNA reverse transcriptase kit (Applied Biosystems). A StepOne Plus real-time PCR system (Applied Biosystems) was used to perform quantitative real-time PCR (qRT-PCR) of cDNA samples using SYBR Select Master mix (Thermo Fisher Scientific). Primer sequences for target genes were used for quantitative PCR amplification of total cDNA. All primers were purchased from Applied Biosystems. For the glioblastoma samples, the following primers were used: RNA18S – GATGGGCGGCGGAAAATAG and GCGTGGATTCTGCATAATGGT, TIPARP – CACCCTCTAGCAATGTCAACTC and CAGACTCGGGATACTCTCTCC. Differences in cDNA input were corrected by normalizing signals obtained with specific primers for 18S rRNA. Relative quantitation of target cDNA was determined by the formula $2^{-\Delta CT}$, with ΔCT denoting fold increases above the set control value. Data was analyzed using StepOnePlus™ (Applied Biosystems), Excel, and Prism.

2.17. Stable isotope tracing

Murine $CD4^+CD25^-$ Tconv cells were stimulated overnight (Figure 4, 5) or for three days (Figure 5) with CD3ε/CD28 mAb-coated beads and 25 U × mL^{-1} IL-2. For labelling we acquired media without background glucose and glutamine. We used Seahorse XF DMEM medium (cat. #102353-100, Agilent) with dialyzed foetal bovine serum (FBS, cat. #26400036, Thermo Fisher Scientific). We added 10 mM $NaHCO_3$ buffer as well as unlabelled glucose and glutamine as needed for controls. For labelling, we used 60 mg × dL^{-1} [$^{13}C_6$] D-glucose (3.3 mM), 6 mM [$^{13}C_5$] L-glutamine, or 0.1 mM [$^{13}C_{16}$] palmitate (CLM-1396-PK, CLM-1822-H-PK, and CLM-409-PK, respectively, all from Cambridge Isotope Laboratories). The [$^{13}C_{16}$] palmitate was dissolved in bovine serum albumin (Sigma Aldrich, cat. #A9205) as an intermediary step prior to being added to the cell culture medium at a final concentration of 0.1 mM. Cells were exposed to labelling media for three hours prior to metabolite extraction.

2.18. Treg function and induction, T cell cytokine production

For Treg suppression assays, purified Tconv cells were labelled with carboxyfluorescein succinimidyl ester (CFSE) or CellTrace Violet (both Thermo Fisher) and stimulated with irradiated antigen presenting cells plus CD3ε mAb (1 μg × mL^{-1}, BD Pharmingen). After 72 h, proliferation of Tconv cells, which at that timepoint have become effector T cells, was determined by flow cytometric analysis of CFSE dilution. For conversion to $Foxp3^+$ Tregs, Tconv cells were incubated for 3-5 days with CD3ε/CD28 mAb beads, plus TGF-β (3 ng × mL^{-1}) and IL-2 (25 U × mL^{-1}), and analysed by flow cytometry for $Foxp3^+$ iTreg [32]. For cytokine production, we incubated freshly isolated $CD4^+CD25^-$ Tconv or $CD8^+$ CTL from C57BL/6J mice overnight (37° C, 5% CO_2) in 24-well plates pre−coated with CD3ε and CD28 mAbs (2 μg × mL^{-1} each, incubated at 37° C for 1 hr). In the morning, PMA/ionomycin and GolgiStop reagents were added to reach final concentrations of 50 ng × mL^{-1} phorbol 12-myristate 13-acetate and 1 μM ionomycin (Sigma-Aldrich), and 0.67 μL GolgiStop per mL of medium. L- or D-kynurenine or water control were added at that point as well. Cells were then incubated for 5 additional hours (37° C, 5% CO_2), and harvested for flow cytometry and/or RNA isolation. We used the Fixation/Permeabilization Buffer set from eBioscience for intranuclear staining.

2.19. Tissue kynurenine measurements

In the mouse melanoma model, 3×10^4 B16.F10 tumour cells were injected in 50 μL RPMI with ECM (1:2) subcutaneously in the dorsal region of female 10-18 weeks old C57BL/6J mice (purchased from Charles River). The B16 tumour experiments were performed according to the regulations of the local government of Würzburg, Germany. For the kynurenine measurements in D-kynurenine fed mice, 8-week-old female C57BL/6J mice received 300 mg × kg^{-1} × d^{-1} kynurenine or control chow as outlined above. Serum (100-200 μL) was obtained from live isoflurane-sedated animals using retroorbital bleeding [33]. Tissue collection was obtained in rapid succession after euthanasia within 30 seconds (spleen, liver) up to a minute (intestine, i.e. ascending colon), thigh skeletal muscle (<2 min), and brain (<4 min). Metabolite extraction and quantification was conducted as described above (LC-MS/MS). For the enzymatic tumour L-kynurenine measurements, ova-expressing Ae17 lung mesothelioma [34] cells were grown in RPMI, 10% foetal bovine serum supplemented with 2 mM L-glutamine. We injected 2×10^6 Ae17 tumour cells subcutaneously into the right flank of 6-8 week old female B6/$Rag1^{-/-}$ mice (female gender to avoid in-fighting). After six days, the mice were implanted an Alzet osmotic pump (filled with DMSO), which served as vehicle control during the evaluation of DMSO-soluble drugs and their effect on tumour size and continued for an additional 7-10 days. Tumour volume was measured as previously reported [32]. The DMSO treated tumour samples were then harvested for kynurenine measurements. The tumours were harvested within one minute of euthanasia and immediately frozen in liquid nitrogen. As control tissue, we harvested liver tissue from the same mice after the tumour retrieval was completed. The liver samples were also frozen in liquid nitrogen, and, like the tumours, stored at −80°C. For tissue kynurenine extraction the samples were homogenized, thawed and mixed 1:1 with 0.5 M metaphosphoric acid (HPO_3) to facilitate deproteinization (limiting artifacts from lactate production/ consumption during sample preparation). Samples were then centrifuged at 10,000 g for 5 min at 4°C. Subsequently, the sample was neutralized by adding 2.2 μL $KHCO_3$, again centrifuged (10,000 g, 5 min, 4°C), and then diluted 1:1 with 50 mM K_2HPO_4, pH 7.5) prior to analysis of L-kynurenine using an ELISA kit (cat# BA-E-2200, ImmuSmol, Bordeaux, France) per the manufacturer's instructions. In brief, the deproteinized samples were placed in a 96-well plate with standards and controls, were exposed to an acylation reagent and kynurenine antiserum, and incubated overnight at 4°C protected from light. On the next day, the plate was washed and exposed to goat anti-rabbit immunoglobulin conjugated with peroxidase and incubated for 30 min at room temperature while on a shaker. After additional washing, a chromogenic substrate containing tetramethylbenzidine was added and the plate was incubated for 25 min at room temperature. Subsequently, the reaction was stopped

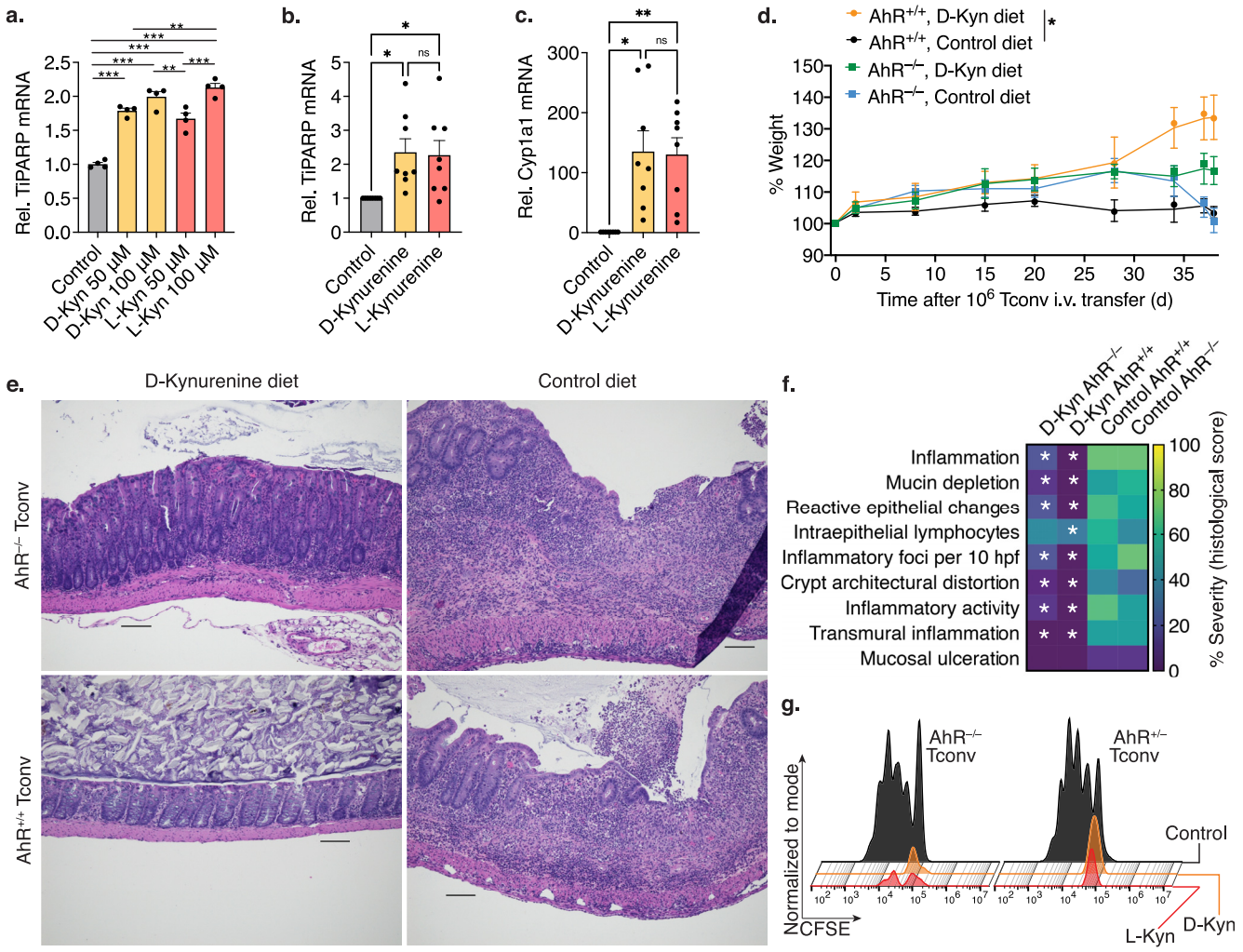

Figure 3. D- and L-Kynurenine activate AhR signalling which mediates part but not all of the immunosuppressive T cell response. (**a-c**) AhR-depedent gene expression via qPCR. Both D- and L-kynurenine invoke AhR signalling in glioblastoma cells (**a**) as well as in co-stimulated Tconv (**b, c**). (**a**) 3/group, one-way ANOVA (**b, c**) 8/group, paired Student t-test. (**d**) B6/Rag1$^{-/-}$ colitis as in Figure 2D with 10^6 AhR$^{+/+}$ and AhR$^{-/-}$ adoptively transferred Tconv (5/group, area under the curve, one-way ANOVA). (**e, f**) Representativetissue sections and blinded colitis histology scoring. (**e**) Colonic specimens from B6/Rag1$^{-/-}$ mice after colitis induction via adoptive Tconv transfer. Specimens from mice receiving control rather than D-kynurenine diet show significant colitis. The beneficial effect of D-kynurenine is diminished if the adoptively transferred Tconv lack AhR. Haematoxylin and eosin staining; scale bar 100 μm. (**f**) Heatmap of blinded histological scoring normalized to a percent scale (two-way ANOVA, 5/group, * indicates $p<0.05$ relative to control diet and AhR$^{+/+}$ Tconv cell condition). (**g**) AhR$^{+/-}$ and AhR$^{-/-}$ Tconv were CFSE-labelled and co-stimulated with or without 1 mM L- and D-kynurenine for three days. Absence of AhR did not protect T cells from apoptosis. *, **, and *** indicate $p<0.05$, $p<0.01$, and $p<0.001$,respectively. Error bars indicate SEM.

with 0.25 M sulfuric acid, and absorbance was read within 10 minutes using a Spectramax Gemini XPS plate reader set to a wavelength of 450 nm. Data was analysed using SoftMax Pro 4.7 software (Molecular Devices, Sunnyvale, CA), MS Excel, and Prism.

2.20. Statistical analysis

Statistical analysis was performed using GraphPad Prism 8 software. Data were tested for normality using the Shapiro-Wilk or Kolmogorov-Smirnov test. Normally distributed data were displayed as mean ± standard error of the mean (SEM), non-normally distributed data as median ± interquartile range (IQR) or range unless otherwise noted. Measurements between two groups were performed with an unpaired Student-t test if normally distributed, or Mann-Whitney U test if otherwise. For paired samples, we used a paired Student-t test or Wilcoxon matched-pairs signed rank test, depending on whether data was normally distributed, respectively. Survival was assessed using Log-rank (Mantel-Cox) testing. Groups of three or more were analysed by one-way and two-way analysis of variance (ANOVA) or the Kruskal-Wallis test, followed by Dunn's or Tukey's multiple comparison test.

2.21. Role of Funders

Funding organizations had no role in study design, data collection, data analyses, interpretation, or writing of this report.

3. Results

3.1. D-kynurenine induces T cell apoptosis in vitro similar to L-kynurenine

D-kynurenine is reportedly not metabolized by kynureninase [16,17], thus precluding the generation of anthranilic acid and its derivative quinolinic acid (**Figure 1a**). We exposed CD3ε/CD28 mAb co-stimulated murine CD4$^+$CD25$^-$ conventional T cells to 1 mM D- or L-kynurenine for three hours and extracted intracellular metabolites. We observed that either kynurenine enantiomer was taken up by

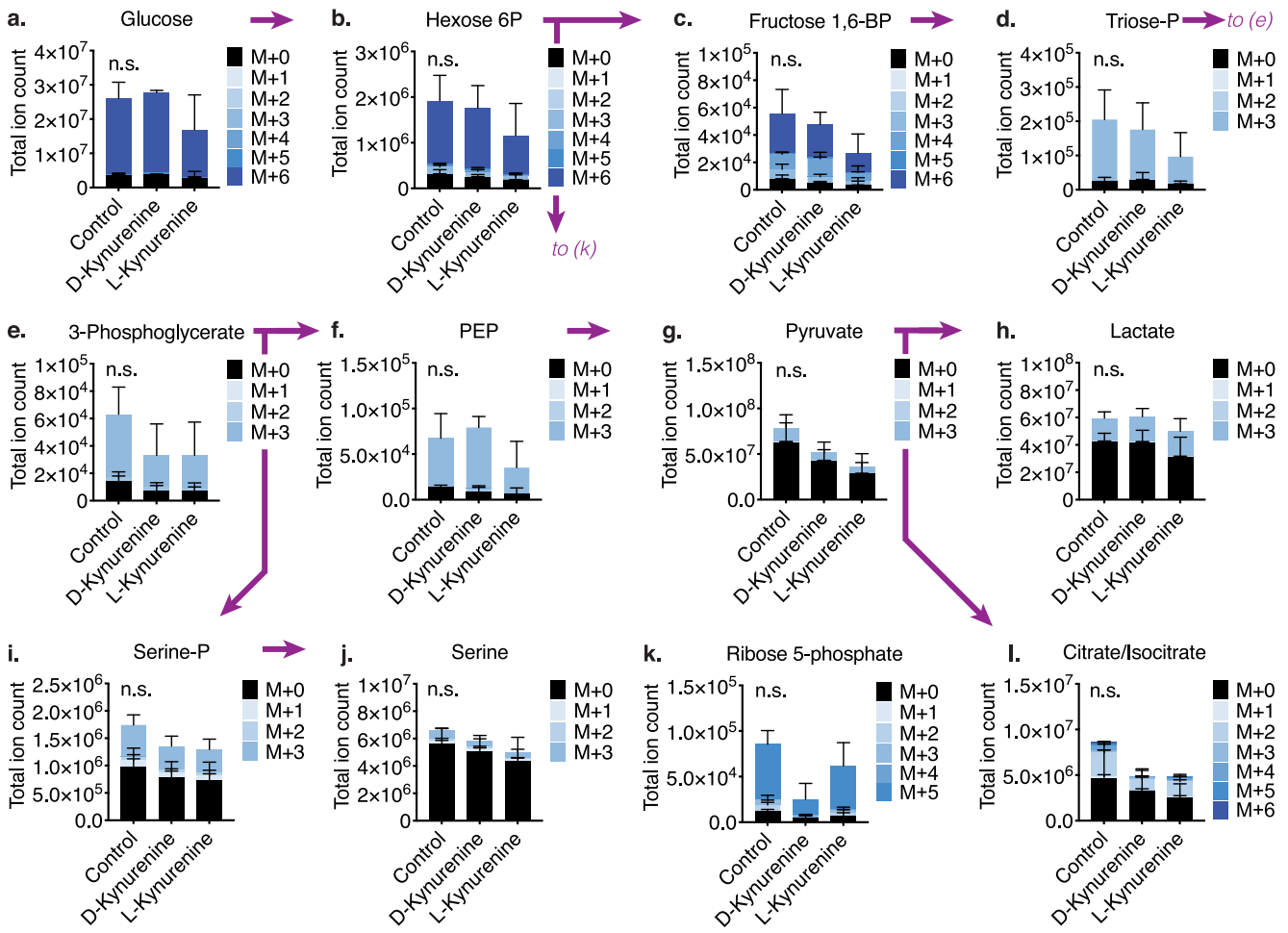

Figure 4. D- and L-kynurenine do not significantly alter glycolytic flux. Tconv were co-stimulated with CD3ε/CD28 mAb-coated beads for 20 hours and were then cultured with [$^{13}C_6$] D-glucose for three hours with either 1 mM of L- or D-kynurenine. Metabolites were extracted and analysed for derivative analysis, with M+1-6 indicating the number of [^{13}C]-atoms per isotopologue (3/group, one-way ANOVA). (**a-h**) Glucose and glucose-derived glycolytic intermediates were not significantly altered by the addition of L- or D-kynurenine. (**i-l**) Likewise, kynurenine treatment did not alter glucose-derived contributions to serine production (**i, j**), the pentose phosphate pathway (**k**), and the Krebs cycle (**l**). Error bars indicate SEM.

stimulated T cells (**Figures 1b, c & S1a**). Like L-kynurenine, D-kynurenine suppressed murine T cell proliferation, which was primarily driven by dose-dependent T cell apoptosis (**Figures 1d, e**). We made similar observations in human CD4$^+$ and CD8$^+$ T cells treated with kynurenine, which underwent apoptosis following CD3ε/CD28 co-stimulation (**Figures 1f, g**), and in mixed leukocyte reactions (**Figures S1b, c**). In addition to T cell proliferation, we observed that both L- and D-kynurenine impaired IFN-γ cytokine production by murine and human CD8$^+$ T cells (**Figures S1d-f**). Similar to proliferation, the decline in IFN-γ production overlapped with cell death (**Figure S1g**). L-kynurenine has been suggested to induce Foxp3$^+$ Treg cells [5], thereby contributing to IDO facilitated suppression of the anti-tumour immune response. We did not observe D- or L-kynurenine to mediate Foxp3$^+$ Treg induction or preferential Foxp3$^+$ Treg survival (**Figures 1h, i & S1i, j**). Likewise, when mixing natural Foxp3$^+$ Treg and effector T cells (Teff), both were subject to similar rates of kynurenine-mediated apoptosis (**Figure S1h**). Taken together, D-kynurenine impairs the ability of T cells to proliferate and function by inducing apoptosis in vitro.

3.2. D-Kynurenine treatment inhibits T cell proliferation in vivo

To further analyse the effect of kynurenines on T cell proliferation, we adoptively transferred 1 $\times$ 10^6 CD4$^+$CD25$^-$ conventional T cells (Tconv) into B6/Rag1$^{-/-}$ mice through intraperitoneal (i.p.) injection; after a week, we started 30 mg/kg/d of D- or L-kynurenine (or water control) i.p. injections (**Figures 2a-c**). We observed, that both D- and L-kynurenine led to an impairment of homeostatic CD4$^+$ T cell proliferation. Next, we intravenously injected B6/Rag1$^{-/-}$ mice with C57BL/6J 1 $\times$ 10^6 Tconv cells to induce autoimmune colitis [25]. As an alternative to kynurenine injections, enteral intake of kynurenine via dietary supplementation can achieve more stable and continuous dosing [35]. We therefore enriched D-kynurenine in mouse chow and fed mice with either 300 mg/kg/d D-kynurenine or control diet and observed that only control diet fed mice lost weight and developed colitis (**Figures 2d, e**). The mice receiving D-kynurenine accumulated kynurenic acid rather than anthranilic acid in brain tissue (**Figure S2a-c**). We did not perform neurologic testing in the kynurenine-fed mice. Colon histology showed reduced inflammation if adoptively transferred B6/Rag1$^{-/-}$ mice received the D-kynurenine chow (**Figures 2f, g, S2d**). Similar to the homeostatic proliferation experiments, we observed reduced spleen CD4$^+$ T cell counts, less activated CD4$^+$ T cells, and no difference in Foxp3$^+$CD4$^+$ Treg (**Figures 2h-k**). The Rag1$^{-/-}$ adoptive transfer colitis is driven by homeostatic T cell proliferation. To evaluate D-kynurenine in more stringent immune challenges, we tested if D-kynurenine treatment could suppress immune responses in dextran sodium sulphate (DSS-) induced colitis as well as in a fully antigen mismatched heart

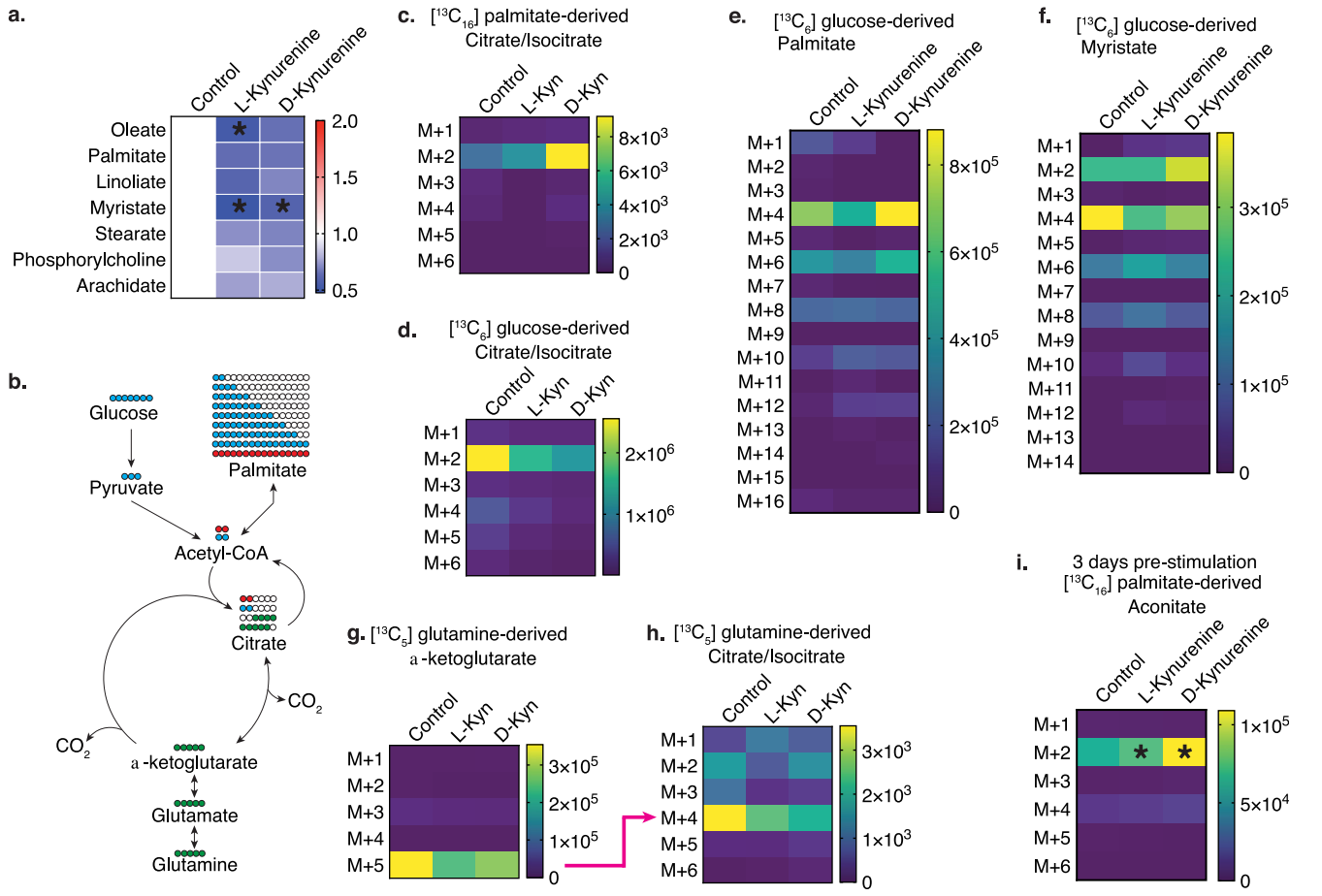

Figure 5. D- and L-kynurenine induce free fatty acid catabolism in T cells. (**a**) Free fatty acid relative total ion counts normalized to control. Data pooled from six independentexperiments (one-way ANOVA). (**b**) Experimental design for [^{13}C] tracing studies to track the fate of carbons derived from added glucose (blue), glutamine (green) or palmitate (pink). (**c-i**) Tconv T cells were co-stimulated overnight (**c-h**) or three days (**i**) and cultured with [$^{13}C_{16}$] palmitate (**c, i**), [$^{13}C_6$] D-glucose (**d-f**), or [$^{13}C_5$] L-glutamine (**g, h**) for three hours ±1 mM L-/D-kynurenine or water control. Metabolites were extracted and analysed for derivative analysis and displayed as heatmaps showing total ion counts, with M+1-16 indicating the number of [^{13}C]-atoms per isotopologue. Data pooled from two (**c, g, h**), three (**i**) and four (**d-f**) independent experiments (two-way ANOVA with Benjamini, Krieger and Yekutieli FDR correction, **a, d-f, i**). * indicates $p<0.05$ to control.

transplant model. Here, we observed that dietary 300 mg/kg/d D-kynurenine administration could neither mitigate DSS-induced colitis (**Figure 2l**) nor delay BALB/c to C57BL/6J cardiac transplant rejection (**Figure 2m**). In conclusion, 300 mg/kg/d D-kynurenine treatment could impair T cell proliferation in vivo and alleviate Rag1$^{-/-}$ autoimmune colitis, but it failed to mitigate DSS-induced colitis and fully mismatched cardiac allograft rejection.

3.3. The aryl hydrocarbon receptor is required for in vivo but not in vitro D-kynurenine effects

L-kynurenine has been identified as an aryl hydrocarbon receptor (AhR) agonist, and as a potential mediator of T cell suppression in vivo. We observed, that both D- and L-kynurenine upregulated the AhR -dependent gene, TiPARP (Tetrachlorodibenzo-p-dioxin (TCDD)-inducible poly(ADP-ribose) polymerase), which is also known as PARP7 or ARTD14, in glioblastoma cells (**Figure 3a**). We have made similar observations of AhR mediated gene upregulation in stimulated Tconv cells exposed to D- and L-kynurenine (**Figures 3b, c**). Based upon this data, as well as reports of the immunosuppressive effects of AhR agonists [36], we questioned if D-kynurenine in vivo treatment would still work if the AhR was absent on T cells. To test this hypothesis, we utilized AhR$^{-/-}$ and AhR$^{+/+}$ control conventional T cells for adoptive transfer colitis (**Figure S3**). We observed that B6/Rag1$^{-/-}$ recipients of AhR$^{-/-}$ CD4$^+$ T cells were less responsive to D-kynurenine treatment in suppressing adoptive transfer colitis relative to AhR$^{+/+}$ CD4$^+$ Tconv recipients (**Figures 3d-f**). B6/Rag1$^{-/-}$ recipients of AhR$^{-/-}$ CD4$^+$ T cells still showed an improvement relative to the control diet, as the absence of AhR is restricted to the adoptively transferred T cells (B6/Rag1$^{-/-}$ mice have normal AhR expression). We also subjected AhR$^{-/-}$ and AhR$^{+/-}$ T cells from the same isolation to in vitro kynurenine exposure, where the absence of AhR was not protective (**Figure 3g**). These data suggested that D-kynurenine might mediate at least part of its suppressive effects in vivo via the AhR, albeit absence of AhR did not protect T cells from kynurenine apoptosis in vitro.

3.4. Kynurenine induces T cell free fatty acid oxidation

AhR signalling was reported to affect cellular metabolism by inhibiting glycolysis and increasing lipid oxidation [37]. Given the effect of kynurenine on AhR signalling, we investigated how kynurenine treatment altered T cell metabolism. We monitored baseline bioenergetic function in co-stimulated murine and human CD4$^+$ T cells exposed to kynurenine. We observed a decline in both oxygen consumption and extracellular acidification (**Figure S4**); however, in this experimental setting, it is difficult to discern cell death from a metabolic switch leading to decreased oxygen consumption or extracellular acidification. To overcome this problem, we utilized [^{13}C] tracing and derivative analysis. To examine glycolysis, we activated

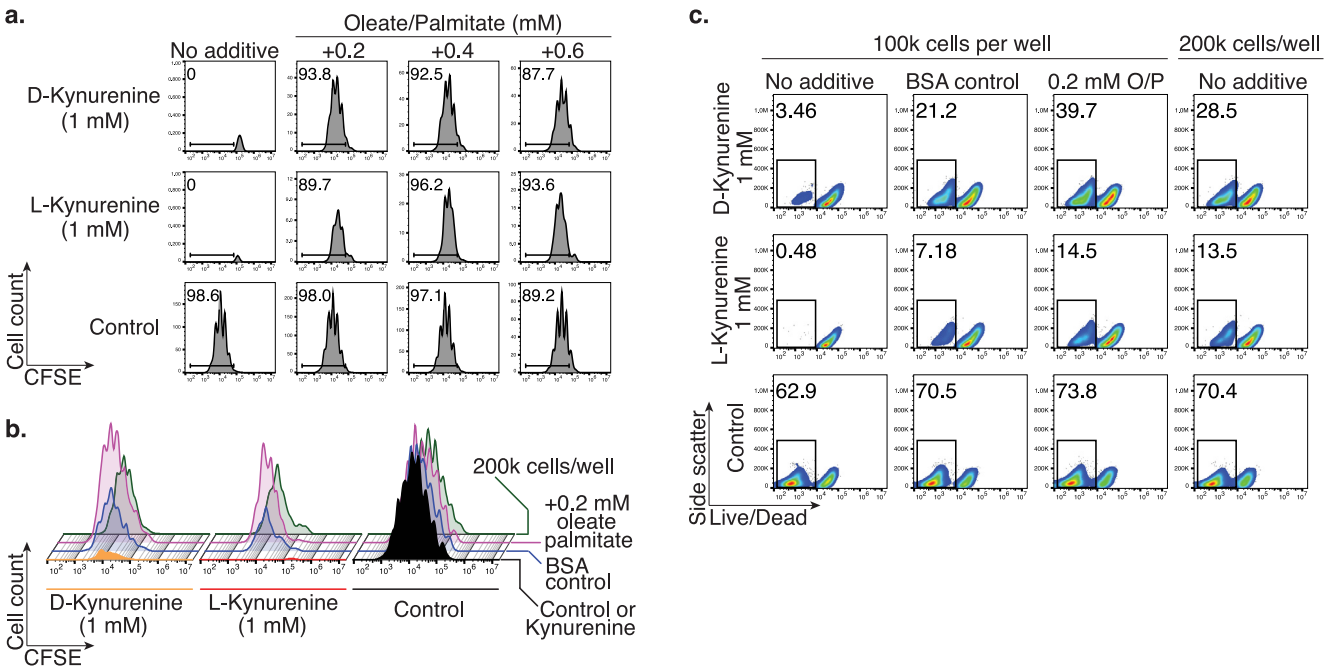

Figure 6. Addition of oleate/palmitate rescues the kynurenine-induced T cell apoptosis phenotype. Murine Tconv were stimulated with CD3ε/CD28 mAb-coated beads $\pm$1 mM L- or D-kynurenine for three days and proliferation assessed through CFSE-dilution. (**a**) Addition of oleate/palmitate rescued Tcell proliferation from kynurenine-induced T cell apoptosis. Data representative of three independent experiments. (**b, c**) Similar to the addition of oleate/palmitate, use of lipid-free bovine serum albumin (vehicle control for oleate/palmitate) and using 2×10^5 instead of 10^5 Tconv per well (200 μL) partially rescued the T cell proliferation (**b**) and apoptosis (**c**) phenotype induced by kynurenine exposure. Data representative of three independent experiments.

murine CD4$^+$ T cells with CD3ε/CD28 mAb-coated beads overnight and cultured the stimulated T cells with [$^{13}C_6$] D-glucose while also exposing them to 1 mM L- or D-kynurenine for three hours. We observed that glycolysis and pyruvate reduction to lactate remained intact (**Figures 4a-h**). Likewise, glucose-derived serine production, which was shown to be important for T cell proliferation [38] and is vulnerable to lactate-induced reductive stress [14], was not affected by kynurenine (**Figures 4i, j**), and neither was the glucose contribution to ATP (**Figure S5a**). Glucose-derived contributions to ribose 5-phosphate and the Krebs cycle trended lower, though the changes did not reach statistical significance (**Figures 4k, l**).

In contrast to glycolytic metabolites, we noted in the same samples, that free fatty acids were reduced after three hours of D- or L-kynurenine exposure (**Figure 5a**). This pattern was not observed for other metabolites such as amino acids and nucleotides (**Figures S5b, c**). We questioned if the decline in free fatty acids was mediated by reduced fatty acid synthesis or increased fatty acid oxidation. We interrogated fatty acid synthesis through [$^{13}C_6$] D-glucose and [$^{13}C_5$] L-glutamine tracing, and fatty acid catabolism through [$^{13}C_{16}$] palmitate tracing (**Figure 5b**). We stimulated CD4$^+$ T cells with CD3ε/CD28 mAb-coated beads overnight, and then labelled cells with either tracer $\pm$1 mM L- or D-kynurenine. We observed that [$^{13}C_{16}$] palmitate labelling led to increased M+2 citrate in the kynurenine-treated conditions (**Figure 5c**). The citrate M+2 trended opposite in the heavy glucose tracing conditions, with kynurenine rather decreasing its formation (**Figures 4k, 5d**). Glucose-derived M+2 citrate can be further traced to free fatty acid biosynthesis, as the citrate shuttle is utilized to deliver acetyl-CoA building blocks into the cytosol for fatty acid biosynthesis (**Figure 5b**). We observed that glucose labelling led to an expected even-numbered isotopologue labelling pattern in palmitate and myristate representing the incorporation of labelled glucose-derived 2-carbon acetate (**Figures 5e, f**). We did not identify a decrease in free fatty acid synthesis in the kynurenine-treated conditions.

Similar to glycolysis, the contributions of [$^{13}C_5$] L-glutamine to the Krebs cycle were not enhanced with kynurenine treatment. As expected, M+5 α-ketoglutarate isotopologue was formed by deamination (**Figure 5g**). After deamination, α-ketoglutarate can contribute to citrate either through the oxidative Krebs cycle (losing one labelled carbon, gaining two unlabelled carbons, resulting in M+4 citrate), or through the reductive Krebs cycle (gaining one unlabelled carbon to yield M+5 citrate) [39]. Kynurenine treatment did not alter the direction of the Krebs cycle, with M+4 citrate being the heavy glutamine-derived predominant isotopologue (**Figure 5h**). Glutamine tracing was not detectable in fatty acids (data not shown). Since M+2 citrate isotopologue was increased with palmitate labelling, we repeated the experiment after three days of stimulation. At this stage, T cells were proliferating and depended on free fatty acids for cell membrane production [40]. We observed that [$^{13}C_{16}$] palmitate labelling led again to increased M+2 aconitate and M+2 citrate isotopologues (**Figures 5i, S5d**). Taken together, the data points towards increased free fatty acid β-oxidation rather than reduced fatty acid synthesis as the cause of decreased free fatty acid levels in T cells after three hours of kynurenine exposure.

3.5. Lipid supplementation rescues kynurenine-induced T cell apoptosis

Our observation of kynurenine-induced fatty acid β-oxidation and depletion further substantiated our suspicion that the prominent kynurenine apoptosis seen in vitro may be an artifact that does not reflect how kynurenine suppresses T cell proliferation in vivo. Since most standard cell culture media do not contain added lipids beyond their serum component, we conducted lipid rescue experiments in which we supplemented an oleate/palmitate mix to our cell culture media. We observed that 0.2 mM of oleate/palmitate rescued murine CD4$^+$ T cell proliferation (**Figure 6a**). Interestingly, we saw a partial rescue effect when adding lipid-free bovine albumin to the cell culture media, which functions as oleate/palmitate vehicle control (**Figure 6b**). In addition, doubling the starting T cell number had a

similar effect on mitigating the apoptosis inducing effects of kynurenine (**Figures 6b, c**). We made similar observations in human $CD4^+$ T cells, where either increasing the serum content from 2% to 10% (**Figure S6a**), or adding oleate/palmitate, albumin, or doubling the starting cell number mitigated kynurenine-induced cell death (**Figure S6b**). Taken together, in vitro T cell apoptosis induced by D- or L-kynurenine can be mitigated by adding oleate/palmitate, increasing free fatty acid transport, or increasing the total number of cells.

3.6. Human tumour tissue kynurenine is present in low micromolar range

Given the failure of IDO-inhibitor treatments in human cancer [10], we questioned if the kynurenine concentration in tumour tissue reaches similar concentrations compared to the 1 mM kynurenine required in our in vitro studies (**Figure 1d-g**). We investigated two immunosuppressive human cancers, renal clear cell carcinoma and head and neck squamous cell carcinoma, which both have known IDO expression and reported increased kynurenine: tryptophan ratios [8,41]. Patient tumour characteristics are summarized in **Table 2**. We observed that the tumour tissue concentrations of kynurenine were higher than in normal kidney or healthy mucosa tissue, but far below levels that were suppressive in vitro (**Figures 7a, b, S7**). In addition to the human tumour data, we also measured mouse B16F10 melanoma (**Figure 7c**) and Ae17 murine mesothelioma (**Figure 7d**), which yielded similarly low measurements. Interestingly, the oral 300 mg/kg/d D-kynurenine therapy utilized above achieved very similar if slightly higher tissue and serum kynurenine concentrations compared to the human tumours (**Figure 7e**). 3-OH kynurenine was measured <0.4 pmol mg^{-1} in all human tumour tissues, and at up to 2 pmol mg^{-1} in the D-kynurenine fed animals (**Figure S7b, e, g**). Taken together, our data show that the kynurenine concentration in human tumours was two orders of magnitude below the apoptosis-inducing in vitro concentration.

Table 2
Patient characteristics and tumour staging and grading

Renal cell carcinoma (RCC)			
Age	Sex	Type	Stage & Grade
63	M	Clear cell carcinoma	$pT_{1a}G_2L_0V_0R_0$
57	M	Clear cell carcinoma	$pT_{1a}G_2L_0V_0R_0$
64	M	Clear cell carcinoma	$pT_{1a}G_2L_0V_0R_0$
69	M	Clear cell carcinoma	$pT_2G_2L_0V_1R_0$
71	M	Clear cell carcinoma	$pT_{2a}G_2L_0V_0R_0$
69	F	Clear cell carcinoma	$pT_{2a}pN_0L_0V_0R_0$
Head and neck squamous cell carcinoma (HNSCC)			
Age	Sex	Type	Stage & Grade
53	M	Oral squamous cell carcinoma	$ypT_2ypN_0cM_0L_0V_0R_0\ Pn_0$
52	M	Oral squamous cell carcinoma	$pT_3pN_1cM_{1(Os\ ilium)}L_0V_0R_0Pn_0G_2$
73	F	Laryngeal carcinoma	$pT_{4a}pN_1cM_0L_1V_1R_0Pn_0G_3$
61	M	Oral squamous cell carcinoma	$pT_3pN_1cM_0L_0V_0R_0Pn_0G_2$
80	F	Oropharyngeal carcinoma	$pT_1pN_0cM_0L_0V_0R_0Pn_0G_2$
71	M	Oropharyngeal carcinoma	$pT_1pN_{3b}cM_0L_1V_1R_0Pn_0G_2$
74	F	Oropharyngeal carcinoma	$pT_{4a}pN_0cM_0L_0V_0R_1Pn_1G_3$
44	M	Oropharyngeal carcinoma	$pT_1pN_0cM_0L_0V_0R_0Pn_0$
62	M	Oropharyngeal carcinoma	$pT_3pN_0cM_0L_0V_0R_0Pn_0G_2$
60	M	Laryngeal carcinoma	$pT_{4a}pN_{3b}cM_0L_1V_0R_0Pn_0G_2$
66	M	Oropharyngeal carcinoma	$pT_{4a}pN_0cM_0L_0V_0R_0Pn_0G_3$
48	F	Oral squamous cell carcinoma	$pT_2pN_1cM_0L_0V_0R_0Pn_0G_2$
67	M	Oral squamous cell carcinoma	$pT_2cN_0cM_0L_0V_0R_0Pn_0G_1$
68	M	Oral squamous cell carcinoma	$pT_2pN_1cM_0L_0V_0R_0Pn_0G_2$
77	M	Hypopharyngeal carcinoma	$pT_{4a}pN_1cM_0L_1V_0R_0Pn_0G_2$
66	M	Oropharyngeal carcinoma	$rpT_3cM_0L_0V_0R_0Pn_0G_3$
73	F	Hypopharyngeal carcinoma	$pT_3L_0V_0pN_0cM_0G_3R_0$
52	M	Oropharyngeal carcinoma	$pT_2pN_{2b}cM_0L_0V_0R_0Pn_0G_2$
63	M	Hypopharyngeal carcinoma	$rpT_{4a}rpN_{2c}cM_0L_0V_0R_0Pn_1G_3$
58	F	Oral squamous cell carcinoma	$pT_2pN_{3b}cM_0L_0V_0R_0Pn_1G_3$
70	M	Hypopharyngeal carcinoma	$pT_2pN_{3b}cM_0L_1V_0R_0Pn_0G_2$
56	M	Laryngeal carcinoma	$pT_2pN_{3b}cM_0L_1V_1R_0Pn_0G_3$
63	F	Oral squamous cell carcinoma	$pT_2pN_{2a}cM_0L_1V_1R_0Pn_1G_2$
67	M	Oral squamous cell carcinoma	$pT_2pN_0cM_0L_0V_0R_0Pn_0G_3$
76	M	Oropharyngeal carcinoma	$pT_3pN_0cM_0L_0V_0R_0Pn_0G_3$
63	M	Oropharyngeal carcinoma	$pT_2pN_0cM_0L_0V_0R_0Pn_0G_2$
64	F	Oropharyngeal carcinoma	$pT_3pN_{2c}cM_0L_1V_0R_0Pn_0G_2$

4. Discussion

When evaluating kynurenine as an immunosuppressive metabolite for potential supplemental immunosuppressive therapy, we found that both L- and D-kynurenine demonstrate immunosuppressive effects in vivo. However, despite reaching tissue and serum kynurenine concentrations at or above those of human cancer patients, the in vivo immunosuppressive effects were weak. Mismatched cardiac allograft rejection was unaffected by kynurenine intake, suggesting that this is not a suitable strategy for therapeutic immunosuppression. Interestingly, our tissue kynurenine measurements revealed that the human tumour kynurenine concentrations were only in the low micromolar range, far below the required 1 mM L- or D-kynurenine needed to induce T cell apoptosis in vitro. Similar to the human tumour kynurenine, we found its derivative 3-OH kynurenine, which also mediates T cell apoptosis and immunosuppression [2,42], was equally well below its reported apoptosis threshold of 100 μM. These observations raise the question whether the inefficacy of IDO inhibitors in human cancer clinical trials [10,43] was due to tissue levels of kynurenine and its derivatives that were too low to act as a major metabolic barrier to anti-tumour immunity. In addition, glioblastoma IDO has also been reported to have non-enzymatic immunosuppressive effects independent of kynurenine [44]. Taken together, low micromolar tumour kynurenine concentrations may have limited immunosuppressive effects which could be clinically important as there is a continuously strong interest in IDO targeting for cancer treatment [45] and ongoing clinical trials with IDO inhibitors [46]. Additional patient stratification may be necessary to identify patients that are more likely to respond to IDO inhibition [47].

In addition to the low tumour tissue kynurenine levels, and the modest immunosuppressive effects induced when feeding mice to achieve comparable concentrations, our study also identifies a potential in vitro artifact that may lead to overestimation of kynurenine-induced T cell apoptosis. Our [$^{13}C_{16}$] palmitate tracing data, as well as the lipid and serum rescue of the T cell apoptosis phenotype support that exposure to L- and D-kynurenine induces free fatty acid catabolism. This can be a problem in standard RPMI tissue culture media, in which fatty acids are typically present in small amounts through added serum. This may also contribute to the relatively weak in vivo immunosuppressive effects of therapeutic L- and D-kynurenine in our studies where lipids are more abundant in most circumstances. Taken together, this data indicates a more marginal role of kynurenine especially when compared to L-lactic acid. L-lactic acid has a well-defined pathophysiologic role in metabolic tumour-associated immunosuppression [48,49], and is much more concentrated in tumours than kynurenine by three to four orders of magnitude [14,50].

That said, this does not mean that kynurenine plays no role in immunosuppression. First, our $Rag1^{-/-}$ colitis and homeostatic proliferation studies show that by giving kynurenine without altering tryptophan an immunosuppressive effect can be induced. As to the strength of the effect, it is possible that there are other modifying factors. Cancer cells extract lipids from their surroundings [51]. It is conceivable, that competition for free fatty acids may be harsher in the tumour environment than in other tissues. For example, it was shown, that tumour Tregs depend on making their own lipids [52]. Perhaps, under the pressure of lipid sparse conditions kynurenine may have a proportionally stronger effect on proliferating effector and cytotoxic T cells as we observed under low lipid vs. lipid supplemented cell culture conditions. In addition, there is also the factor of tryptophan depletion through IDO/TDO [45]. A decreased

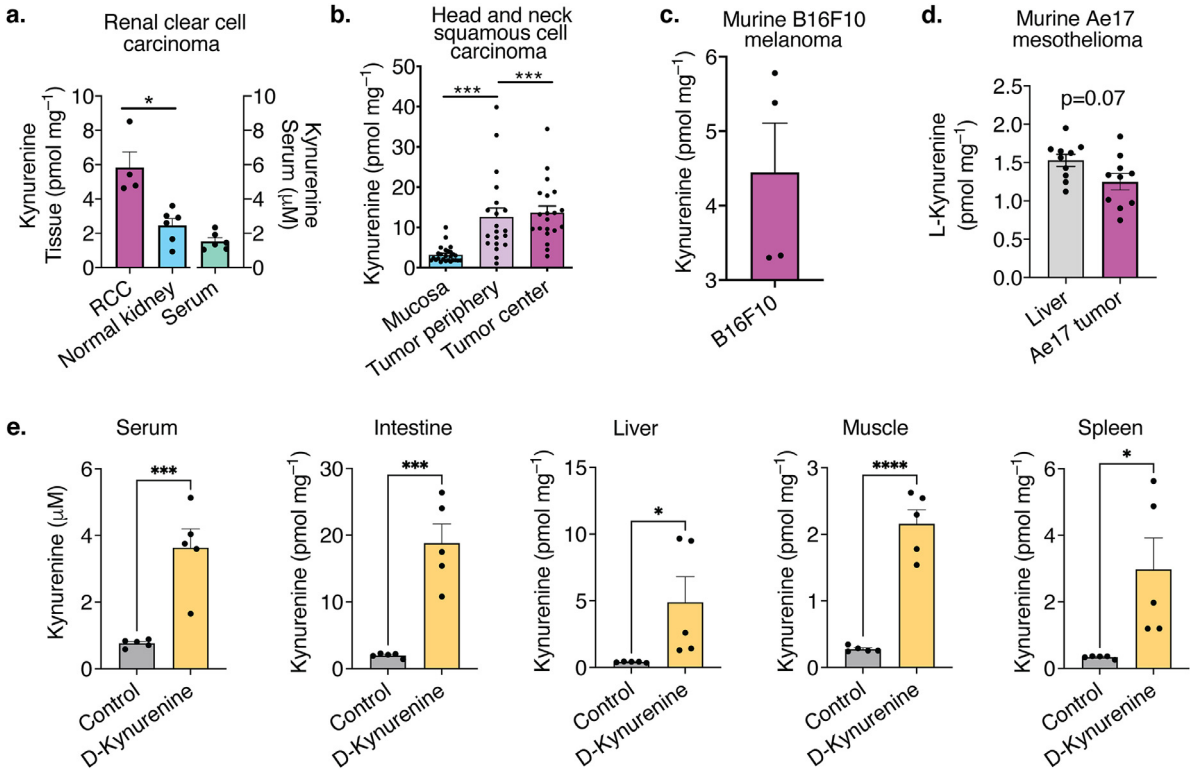

Figure 7. Human renal cell carcinoma and head and neck cancer exhibit low micromolar kynurenine tissue concentrations. (**a, b**) Levels of kynurenine were determined by LC-MS/MS in serum, cancer and healthy tissue frompatients with renal cell carcinoma (**a**) and head and neck squamous cell carcinoma (**b**). Each dot represents an individual patient. (**c, d**) Murine B16F10 (**c**) and Ae17 mesothelioma (**d**) were implantedinto C57BL/6J mice and eventually frozen in liquid nitrogen. Kynurenine was measured by LC-MS/MS(**c**) and enzymatic L-kynurenine specific ELISA (**d**). Each dot represents an individual tumour experiment. (**e**) C57BL/6J mice were fed D-kynurenine enriched (300 mg/kg/d) or control chow for 10 days (5/group). Serum was obtained from living mice, tissue after euthanasia in rapid succession. Metabolites were extracted and measured by LC-MS/MS. (**a, c-e**) Paired Student t-test. (**b**) Paired one-way ANOVA. *, **, ***, and **** indicate $p<0.05$, $p<0.01$, $p<0.001$, and $p<0.0001$, respectively. Error bars indicate SEM.

tryptophan: kynurenine ratio has been recognized as a poor prognostic factor in several cancers, including HNSCC [9]. However, how that is mechanistically linked remains unclear. In our human cancer measurements, tryptophan was either not depleted (HNSCC) or still within the reference range (RCC).

Our study provides additional insights into the role of AhR in mediating kynurenine effects on T cells. Considering that $Rag1^{-/-}$ mice adoptively transferred with $AhR^{-/-}$ T cells were less responsive to D-kynurenine than those that received $AhR^{+/+}$ T cells, the effects appear to be mediated at least in part through AhR signalling. L-Kynurenine has been established as an AhR ligand agonist that is important to tumour growth; gliomas expressing IDO lost their tumour growth advantage in $AhR^{-/-}$ mice [53]. L-kynurenine can induce programmed cell death protein-1 in T cells through AhR [54]. However, there are also structural chemistry data that suggest L-kynurenine to be a weak binding agonist to AhR, and that more potent AhR agonists can be formed from L-kynurenine through aromatic condensation [55]. In addition, other natural, L-kynurenine derived metabolites such as cinnabarinic acid (from 3-hydroxyanthranilic acid) have been reported as AhR agonists with immunological function [56]. We observed that both L- and D-kynurenine are equally well taken up by T cells and that both stimulate the AhR. The [$^{13}C_{16}$] palmitate tracing as well as the lipid and serum rescue of the T cell apoptosis phenotype support that exposure to L- and D-kynurenine induces free fatty acid catabolism. AhR has been suggested to trigger fatty acid oxidation in T cells while an IDO inhibitor suppressed carnitine palmitoyltransferase I expression [37]. Beyond kynurenine, kynurenic acid has been shown to activate fatty acid oxidation through the G protein-coupled receptor 35 [57]. While this might explain the observed increase in fatty acid catabolism even in $AhR^{-/-}$ T cells, kynurenic acid had no effect on T cells in our in vitro studies, thus excluding it as a major effector of immunosuppression.

With regard to the effect of kynurenine on regulatory T cells (Treg), our in vitro studies did not replicate prior observations of enhanced $Foxp3^{+}$ Treg formation [3,5]. We speculate that this may be the result of different in vitro experimental conditions. Our studies have shown how sensitive kynurenine-induced T cell apoptosis was to minor alterations in cell culture serum and lipid content, as well as the number of cells used per well. It is conceivable that $Foxp3^{+}$ Treg formation and stability could be similarly responsive to cell culture conditions. Notably, we did not see an effect on Tregs in vivo in our kynurenine administration experiments either, supporting a limited immunosuppressive role of kynurenine in vivo at the concentrations measured in our tumour samples.

Is it possible to take advantage of kynurenine in supplementation in some form for immunosuppressive therapy? L-kynurenine is unsuitable due to its neurotoxicity [15]. While we hypothesized D-kynurenine might have less neurotoxicity than L-kynurenine, it is important to point out that this report provides no data to support this. Aside from the neurotoxicity question, purely from an immunosuppressive point of view, the case for D-kynurenine is weak. While D-kynurenine could somewhat impair T cell proliferation and alleviate $Rag1^{-/-}$ colitis, it could neither delay MHC-mismatched allograft rejection nor alter the course of DSS-induced colitis. Hence, D-

kynurenine does not appear to be a promising candidate for immunosuppressive therapy.

In conclusion, both L- and D-kynurenine affect T cell lipid catabolism and have demonstratable but ultimately weak immunosuppressive effects in vivo. This may explain the observed inefficacy of IDO inhibitors in human cancer trials. The measured in vivo concentration of kynurenine in human HNSCC and RCC was much lower than the required concentration to suppress in vitro T cell proliferation, which might indicate that the contribution of kynurenine to the suppression of anti-tumour immunity has been overestimated.

Data sharing

All primary data in this study will be made available upon request to the corresponding authors for individuals with appropriate data sharing agreements in place.

Contributors

Conceptualization: UHB, PJS, MK, KS; Investigation: PJS, JJ, KS, CM, MDC, ZW, RSB, KD, PJO, WJQ, LMC, LW, KNO, IU, RM, UHB.; Analysis: PJS, JJ, KS, CM, MDC, BJW, WWH, JAB, MHL, CAO, KR, LZ, MK, UHB; Resources: KR; Writing– Original Draft: UHB; Writing– Review & Editing: PJS, PJO, KD, WWH, JAB, MK.

Declaration of Competing Interest

The authors declare no conflicts of interest.

Acknowledgements

We thank Christiane Opitz (German Cancer Research Centre, Heidelberg, Germany) and Robert Schwarcz (University of Maryland) for advice and helpful comments. We thank the Penn Human Immunology core and the Penn Institute for Diabetes, Obesity & Metabolism for core services. Financial support was as follows: Laffey McHugh foundation and American Society of Nephrology funding (to UHB); DK098656 and AG043483 (to JAB); DK106243 (to MHL); AI073489 and AI095276 (to WWH); Else Kröner-Fresenius-Stiftung (to PJS and IU); DK105562 and AI132391 (to LZ).

Supplementary materials

Supplementary material associated with this article can be found in the online version at doi:10.1016/j.ebiom.2021.103734.

References

[1] Tran MT, Zsengeller ZK, Berg AH, Khankin EV, Bhasin MK, Kim W, et al. PGC1alpha drives NAD biosynthesis linking oxidative metabolism to renal protection. Nature 2016;531(7595):528–32.
[2] Fallarino F, Grohmann U, Vacca C, Bianchi R, Orabona C, Spreca A, et al. T cell apoptosis by tryptophan catabolism. Cell Death Differ 2002;9(10):1069–77.
[3] Fallarino F, Grohmann U, You S, McGrath BC, Cavener DR, Vacca C, et al. The combined effects of tryptophan starvation and tryptophan catabolites down-regulate T cell receptor zeta-chain and induce a regulatory phenotype in naive T cells. J Immunol 2006;176(11):6752–61.
[4] Li L, Huang L, Lemos HP, Mautino M, Mellor AL. Altered tryptophan metabolism as a paradigm for good and bad aspects of immune privilege in chronic inflammatory diseases. Frontiers in immunology 2012;3:109.
[5] Mezrich JD, Fechner JH, Zhang X, BP Johnson, Burlingham WJ, Bradfield CA. An interaction between kynurenine and the aryl hydrocarbon receptor can generate regulatory T cells. J Immunol 2010;185(6):3190–8.
[6] Nguyen NT, Hanieh H, Nakahama T, Kishimoto T. The roles of aryl hydrocarbon receptor in immune responses. International immunology 2013;25(6):335–43.
[7] Sumitomo M, Takahara K, Zennami K, Nagakawa T, Maeda Y, Shiogama K, et al. Tryptophan 2,3-dioxygenase in tumor cells is associated with resistance to immunotherapy in renal cell carcinoma. Cancer Sci 2021;112(3):1038–47.
[8] Seeber A, Klinglmair G, Fritz J, Steinkohl F, Zimmer KC, Aigner F, et al. High IDO-1 expression in tumor endothelial cells is associated with response to immunotherapy in metastatic renal cell carcinoma. Cancer Sci 2018;109(5):1583–91.
[9] Lin DJ, Ng JCK, Huang L, Robinson M, O'Hara J, Wilson JA, et al. The immunotherapeutic role of indoleamine 2,3-dioxygenase in head and neck squamous cell carcinoma: A systematic review. Clin Otolaryngol 2021.
[10] Long GV, Dummer R, Hamid O, Gajewski TF, Caglevic C, Dalle S, et al. Epacadostat plus pembrolizumab versus placebo plus pembrolizumab in patients with unresectable or metastatic melanoma (ECHO-301/KEYNOTE-252): a phase 3, randomised, double-blind study. Lancet Oncol 2019;20(8):1083–97.
[11] Marin E, Bouchet-Delbos L, Renoult O, Louvet C, Nerriere-Daguin V, Managh AJ, et al. Human Tolerogenic Dendritic Cells Regulate Immune Responses through Lactate Synthesis. Cell Metab 2019;30(6):1075–90 e8.
[12] Saez-Lara MJ, Gomez-Llorente C, Plaza-Diaz J, Gil A. The role of probiotic lactic acid bacteria and bifidobacteria in the prevention and treatment of inflammatory bowel disease and other related diseases: a systematic review of randomized human clinical trials. Biomed Res Int 2015;2015:505878.
[13] Angelin A, Gil-de-Gomez L, Dahiya S, Jiao J, Guo L, Levine MH, et al. Foxp3 Reprograms T Cell Metabolism to Function in Low-Glucose, High-Lactate Environments. Cell Metab 2017;25(6):1282–1293.e7.
[14] Quinn WJ, Jiao J, TeSlaa T, Stadanlick J, Wang Z, Wang L, et al. Lactate Limits T Cell Proliferation via the NAD(H) Redox State. Cell Rep 2020;33(11):108500.
[15] Vecsei L, Szalardy L, Fulop F, Toldi J. Kynurenines in the CNS: recent advances and new questions. Nature reviews Drug discovery 2013;12(1):64–82.
[16] Loh HH, Berg CP. Conversion of D-tryptophan to nicotinic acid in the rat. The Journal of nutrition 1971;101(12):1601–6.
[17] Wang XD, Notarangelo FM, Wang JZ, Schwarcz R. Kynurenic acid and 3-hydroxykynurenine production from D-kynurenine in mice. Brain research 2012;1455:1–9.
[18] Santamaria A, Rios C, Solis-Hernandez F, Ordaz-Moreno J, Gonzalez-Reynoso L, Altagracia M, et al. Systemic DL-kynurenine and probenecid pretreatment attenuates quinolinic acid-induced neurotoxicity in rats. Neuropharmacology 1996;35(1):23–8.
[19] Chiarugi A, Carpenedo R, Moroni F. Kynurenine disposition in blood and brain of mice: effects of selective inhibitors of kynurenine hydroxylase and of kynureninase. J Neurochem 1996;67(2):692–8.
[20] Stone TW, Forrest CM, Darlington LG. Kynurenine pathway inhibition as a therapeutic strategy for neuroprotection. FEBS J 2012;279(8):1386–97.
[21] Fernandez-Salguero P, Pineau T, Hilbert DM, McPhail T, Lee SS, Kimura S, et al. Immune system impairment and hepatic fibrosis in mice lacking the dioxin-binding Ah receptor. Science 1995;268(5211):722–6.
[22] Bachmanov AA, Reed DR, Beauchamp GK, Tordoff MG. Food intake, water intake, and drinking spout side preference of 28 mouse strains. Behav Genet 2002;32(6):435–43.
[23] Beier UH, Angelin A, Akimova T, Wang L, Liu Y, Xiao H, et al. Essential role of mitochondrial energy metabolism in Foxp3(+) T-regulatory cell function and allograft survival. FASEB journal: official publication of the Federation of American Societies for Experimental Biology 2015;29(6):2315–26.
[24] Beier UH, Wang L, Bhatti TR, Liu Y, Han R, Ge G, et al. Sirtuin-1 targeting promotes Foxp3+ T-regulatory cell function and prolongs allograft survival. Molecular and cellular biology 2011;31(5):1022–9.
[25] Akimova T, Xiao H, Liu Y, Bhatti TR, Jiao J, Eruslanov E, et al. Targeting sirtuin-1 alleviates experimental autoimmune colitis by induction of Foxp3+ T-regulatory cells. Mucosal immunology 2014;7(5):1209–20.
[26] Okayasu I, Hatakeyama S, Yamada M, Ohkusa T, Inagaki Y, Nakaya R. A novel method in the induction of reliable experimental acute and chronic ulcerative colitis in mice. Gastroenterology 1990;98(3):694–702.
[27] Beier UH, Wang L, Han R, Akimova T, Liu Y, Hancock WW. Histone deacetylases 6 and 9 and sirtuin-1 control Foxp3+ regulatory T cell function through shared and isoform-specific mechanisms. Science signaling 2012;5(229):ra45.
[28] Melamud E, Vastag L, Rabinowitz JD. Metabolomic Analysis and Visualization Engine for LC−MS Data. Analytical Chemistry 2010;82(23):9818–26.
[29] Su X, Lu W, Rabinowitz JD. Metabolite Spectral Accuracy on Orbitraps. Analytical Chemistry. 2017;89(11):5940–8.
[30] Singer K, Dettmer K, Unger P, Schonhammer G, Renner K, Peter K, et al. Topical Diclofenac Reprograms Metabolism and Immune Cell Infiltration in Actinic Keratosis. Front Oncol 2019;9:605.
[31] Zhu W, Stevens AP, Dettmer K, Gottfried E, Hoves S, Kreutz M, et al. Quantitative profiling of tryptophan metabolites in serum, urine, and cell culture supernatants by liquid chromatography-tandem mass spectrometry. Analytical and bioanalytical chemistry 2011;401(10):3249–61.
[32] Xiao H, Jiao J, Wang L, O'Brien S, Newick K, Wang LC, et al. HDAC5 controls the functions of Foxp3(+) T-regulatory and CD8(+) T cells. International journal of cancer Journal international du cancer 2016;138(10):2477–86.
[33] Levine MH, Wang Z, Xiao H, Jiao J, Wang L, Bhatti TR, et al. Targeting Sirtuin-1 prolongs murine renal allograft survival and function. Kidney Int 2016;89(5):1016–26.
[34] Jackaman C, Bundell CS, Kinnear BF, Smith AM, Filion P, van Hagen D, et al. IL-2 intratumoral immunotherapy enhances CD8+ T cells that mediate destruction of tumor cells and tumor-associated vasculature: a novel mechanism for IL-2. J Immunol 2003;171(10):5051–63.
[35] Pocivavsek A, Thomas MA, Elmer GI, Bruno JP, Schwarcz R. Continuous kynurenine administration during the prenatal period, but not during adolescence, causes learning and memory deficits in adult rats. Psychopharmacology (Berl) 2014;231(14):2799–809.
[36] Gutierrez-Vazquez C, Quintana FJ. Regulation of the Immune Response by the Aryl Hydrocarbon Receptor. Immunity 2018;48(1):19–33.
[37] Eleftheriadis T, Pissas G, Liakopoulos V, Stefanidis I. IDO decreases glycolysis and glutaminolysis by activating GCN2K, while it increases fatty acid oxidation by

activating AhR, thus preserving CD4+ Tcell survival and proliferation. Int J Mol Med 2018;42(1):557–68.
[38] Ma EH, Bantug G, Griss T, Condotta S, Johnson RM, Samborska B, et al. Serine Is an Essential Metabolite for Effector T Cell Expansion. Cell Metab 2017;25(2):345–57.
[39] Fendt SM, Bell EL, Keibler MA, Olenchock BA, Mayers JR, Wasylenko TM, et al. Reductive glutamine metabolism is a function of the alpha-ketoglutarate to citrate ratio in cells. Nat Commun 2013;4:2236.
[40] Assmann N, Finlay DK. Metabolic regulation of immune responses: therapeutic opportunities. The Journal of clinical investigation 2016;126(6):2031–9.
[41] Solomon B, Young RJ, Rischin D. Head and neck squamous cell carcinoma: Genomics and emerging biomarkers for immunomodulatory cancer treatments. Semin Cancer Biol 2018;52(Pt 2):228–40.
[42] Zaher SS, Germain C, Fu H, Larkin DF, George AJ. 3-hydroxykynurenine suppresses CD4+ T-cell proliferation, induces T-regulatory-cell development, and prolongs corneal allograft survival. Invest Ophthalmol Vis Sci 2011;52(5):2640–8.
[43] Hellmann MD, Gettinger S, Chow LQM, Gordon M, Awad MM, Cha E, et al. Phase 1 study of epacadostat in combination with atezolizumab for patients with previously treated advanced nonsmall cell lung cancer. International journal of cancer Journal international du cancer 2020;147(7):1963–9.
[44] Zhai L, Bell A, Ladomersky E, Lauing KL, Bollu L, Nguyen B, et al. Tumor Cell IDO Enhances Immune Suppression and Decreases Survival Independent of Tryptophan Metabolism in Glioblastoma. Clin Cancer Res 2021.
[45] Tang K, Wu YH, Song Y, Yu B. Indoleamine 2,3-dioxygenase 1 (IDO1) inhibitors in clinical trials for cancer immunotherapy. J Hematol Oncol 2021;14(1):68.
[46] Sonpavde G, Necchi A, Gupta S, Steinberg GD, Gschwend JE, Van Der Heijden MS, et al. ENERGIZE: a Phase III study of neoadjuvant chemotherapy alone or with nivolumab with/without linrodostat mesylate for muscle-invasive bladder cancer. Future Oncol 2020;16(2):4359–68.
[47] Opitz CA, LF Somarribas Patterson, Mohapatra SR, Dewi DL, Sadik A, Platten M, et al. The therapeutic potential of targeting tryptophan catabolism in cancer. Br J Cancer 2020;122(1):30–44.
[48] Siska PJ, Singer K, Evert K, Renner K, Kreutz M. The immunological Warburg effect: Can a metabolic-tumor-stroma score (MeTS) guide cancer immunotherapy? Immunol Rev 2020;295(1):187–202.
[49] Tu VY, Ayari A, O'Connor RS. Beyond the Lactate Paradox: How Lactate and Acidity Impact T Cell Therapies against Cancer. Antibodies (Basel) 2021;10(3).
[50] Walenta S, Wetterling M, Lehrke M, Schwickert G, Sundfor K, Rofstad EK, et al. High lactate levels predict likelihood of metastases, tumor recurrence, and restricted patient survival in human cervical cancers. Cancer research 2000;60(4):916–21.
[51] Corn KC, Windham MA, Rafat M. Lipids in the tumor microenvironment: From cancer progression to treatment. Prog Lipid Res 2020;80:101055.
[52] Lim SA, Wei J, Nguyen TM, Shi H, Su W, Palacios G, et al. Lipid signalling enforces functional specialization of Treg cells in tumours. Nature 2021.
[53] Opitz CA, Litzenburger UM, Sahm F, Ott M, Tritschler I, Trump S, et al. An endogenous tumour-promoting ligand of the human aryl hydrocarbon receptor. Nature 2011;478(7368):197–203.
[54] Liu Y, Liang X, Dong W, Fang Y, Lv J, Zhang T, et al. Tumor-Repopulating Cells Induce PD-1 Expression in CD8(+) T Cells by Transferring Kynurenine and AhR Activation. Cancer Cell 2018;33(3):480–94 e7.
[55] Seok SH, Ma ZX, Feltenberger JB, Chen H, Chen H, Scarlett C, et al. Trace derivatives of kynurenine potently activate the aryl hydrocarbon receptor (AHR). The Journal of biological chemistry 2018;293(6):1994–2005.
[56] Lowe MM, Mold JE, Kanwar B, Huang Y, Louie A, Pollastri MP, et al. Identification of cinnabarinic acid as a novel endogenous aryl hydrocarbon receptor ligand that drives IL-22 production. PloS one 2014;9(2):e87877.
[57] Agudelo LZ, Ferreira DMS, Cervenka I, Bryzgalova G, Dadvar S, Jannig PR, et al. Kynurenic Acid and Gpr35 Regulate Adipose Tissue Energy Homeostasis and Inflammation. Cell Metab 2018;27(2):378–92 e5.